This article has not been copyedited and formatted. The final version may differ from this version.
JPET Fast Forward. Published on February 27, 2006 as DOI: 10.1124/jpet.105.099507

JPET #99507

LOCALIZATION OF THE KAPPA OPIOID RECEPTOR IN LIPID RAFTS

Wei Xu, Su-In Yoon, Peng Huang, Yulin Wang, Chongguang Chen,

Parkson Lee-Gau Chong and Lee-Yuan Liu-Chen

Department of Pharmacology, Center for Substance Abuse Research (W.X., P. H., Y. W., C. C., L.-Y. L.-C.), and Department of Biochemistry (S.-I. Y., P.L.-G. C), Temple University School of Medicine, Philadelphia, PA

JPET Fast Forward. Published on February 27, 2006 as DOI: 10.1124/jpet.105.099507
This article has not been copyedited and formatted. The final version may differ from this version.

Running title: The κ opioid receptor and lipid rafts

*Correspondence should be sent to: Dr. Lee-Yuan Liu-Chen, Department of Pharmacology, Temple University School of Medicine, 3420 N. Broad St., Philadelphia, PA 19140,

Phone: (215) 707-4188; fax: (215) 707-7068; e-mail: lliuche@temple.edu

The number of text pages: 42

Number of tables: 1

Figures: 9

References: 60

The number of words in the Abstract: 245

The number of words in Introduction: 749

The number of words in Discussion: 1965

Abbreviations: CHO cells, Chinese hamster ovary cells; FLAG epitope, (DYKDDDDK); FLAG-hKOR, FLAG-tagged human κ opioid receptor; CHO-sFLAG-hKOR, CHO cells stably transfected with FLAG-hKOR cDNA which has a signal peptide preceding the FLAG-hKOR; EDTA, Ethylenediaminetetraacetic acid, DTT, dithiothreitol; PMSF, phenylmethanesulfonyl fluoride; EGTA, ethylene glycol-bis(β–aminoethyl ether)-N,N,N', N'-tetraacetic acid; GPCR, G protein-coupled receptor; hKOR, the human κ opioid receptor; HRP, horseradish peroxidase; MAP kinase, mitogen-activated protein kinase; MCD, methyl β-cyclodextrin; CH-MCD, MCD-conjugated cholesterol; MES, 2-morpholinoethanesulfonic acid; SDS-PAGE, sodium dodecyl sulfate – polyacrylamide gel electrophoresis; TBS-T, 10 mM Tris-HCl, 159 mM NaCl, 0.1 % Tween-20, pH 7.4; TM7, the seventh transmembrane helix; U50,488H, (-)(*trans*)-3,4-dichloro-N-methyl-N-[2-(1-pyrrolidiny) cyclohexyl]benzeneacetamide.

Abstract

Lipid rafts are microdomains of plasma membranes enriched in cholesterol and sphingolipids in the outer layer. We determined if κ opioid receptors (KOR) in human placenta and FLAG-tagged human KOR (FLAG-hKOR) expressed in CHO cells are localized in lipid rafts and if changes in cholesterol contents affect hKOR properties and signaling. Lipid rafts were prepared from placenta membranes and CHO cells expressing FLAG-hKOR using the Na_2CO_3 method of Song et al. (1996) and fractionation through a sucrose density gradient. The majority of the KOR in the placenta and FLAG-hKOR in CHO cells, determined by [^{3}H]diprenorphine binding and/or immunoblotting with an anti-FLAG antibody, was present in low density fractions, coincided with high levels of caveolin-1 and cholesterol, markers of lipid rafts, indicating that the KOR is localized in lipid rafts. Pretreatment with 2% methyl β-cyclodextrin (MCD) reduced cholesterol content by ~48% and changed the cells from spindle-shaped to spherical. MCD treatment disrupted lipid rafts, shifted caveolin-1 and FLAG-hKOR to higher density fractions, increased affinity of U50,488H for the hKOR and greatly increased U50,488H-induced [^{35}S]GTPγS binding and p42/44 MAP kinase phosphorylation. Cholesterol replenishment reversed all the MCD effects. Caveolin-1 immunoprecipitated with $G_{\alpha i}$ proteins and MCD treatment reduced caveolin-1 associated with $G_{\alpha i}$ proteins, which may contribute to the enhanced agonist-induced G protein activation. Caveolin-1 also immunoprecipitated with FLAG-hKOR, but MCD treatment had no effect on the association. Thus, the KOR is located in lipid rafts and its localization in the microdomains greatly impacts on coupling to G proteins.

Introduction:

Plasma membranes were traditionally viewed as uniform lipid bilayers and G protein-coupled receptors (GPCRs), G proteins, and membrane-bound effectors were randomly distributed in plasma membranes. In recent years, the concept that lipid rafts function as microdomains in plasma membranes to concentrate signaling molecules for regulated activation by related receptors has gained increasing acceptance (Pike, 2003; Chini and Parenti, 2004; Cohen et al., 2004). Lipid rafts are microdomains of cell membranes highly enriched in cholesterol and sphingolipids in the outer layer. Brown and Rose (1992) proposed the following operational definition of lipid rafts: when cell membranes were solubilized with cold non-ionic detergents such as Triton X-100 (1% for 1 h at 4°C) followed by sucrose density gradient centrifugation, lipid rafts are resistant to detergent solubilization and float in the lighter fractions, while the bulk of the solublized cellular lipids and proteins are in the high density fractions (Brown and Rose, 1992). There are two types of lipid rafts: planar lipid rafts and caveolae. Caveolae, a specialized subtype of lipid rafts, are flask-shaped invaginations in the plasma membrane and are enriched in caveolins, 21-24-kDa integral membrane proteins (Razani et al., 2002). Many signaling molecules including some GPCRs, G_α proteins, growth factor receptors, protein kinase C, and adenylyl cyclase were found to be enriched in or recruited into lipid rafts (Pike, 2003; Chini and Parenti, 2004). Growing evidence has indicated that lipid rafts are crucial in the regulation of GPCRs in signal transduction and in exocytic and endocytic pathways (Pike, 2003; Chini and Parenti, 2004).

Cholesterol has been shown to play a critical role in assembling microdomains of lipid rafts, binding directly to caveolins and facilitating caveolin integration into membrane (Murata et al., 1995; Li et al., 1996). MCD is used extensively as a cholesterol-depleting reagent, rapidly

removing cholesterol from the plasma membrane of cultured cells (Kilsdonk et al., 1995) and eventually leading to disruption of lipid rafts (Rothberg et al., 1992; Lawrence et al., 2003).

Caveolins have been demonstrated to interact with many signaling molecules, likely through interactions with specific caveolin-binding motifs in the proteins (Okamoto et al., 1998; Cohen et al., 2004). Thus, caveolins may function as scaffolding proteins to concentrate signaling molecules within caveolae membranes. Caveolins were shown to negatively regulate the activities of many signaling molecules (Okamoto et al., 1998). Caveolin-1 and -2 are widely distributed and coexpressed in most differentiated cells (Cohen et al., 2004).

Opioid drugs and endogenous peptides produce pharmacological and physiological effects by acting on at least three types of opioid receptors, μ, δ and κ. Stimulation of κ opioid receptors elicits many effects including analgesia, water diuresis, dysphoria and antipruritic effects and attenuation of cocaine craving in addicts [see (Liu-Chen, 2004) and references therein]. Salvinorin A, a potent hallucinogen extracted from leaves of the plant *Salvia divinorum*, is a potent and selective agonist of the κ opioid receptor (Roth et al., 2002). κ opioid receptors are also present in non-neuronal tissues, including the human placenta (Porthe et al., 1981; Mansson et al., 1994) and the rat heart (Ventura et al., 1989). In the human placenta, κ opioid receptors regulate secretion of human chorionic gonadotropin (Valette et al., 1983) and release of human lactogen (Petit et al., 1991). In the heart, activation of the κ opioid receptor produces negative ionotropic effects and κ agonists have cardio-protective effects (Peart et al., 2005).

Opioid receptors are mainly coupled to G_i/G_o proteins to affect several different effectors, including inhibition of adenylyl cyclase, enhancement of K^+ conductance, decrease in Ca^{++} conductance and activation of p42/p44 mitogen-activated protein (MAP) kinases [for a review, see (Law et al., 2000)]. In addition, opioid receptors are shown to be coupled to Gz and G16

JPET Fast Forward. Published on February 27, 2006 as DOI: 10.1124/jpet.105.099507
This article has not been copyedited and formatted. The final version may differ from this version.

(Law et al., 2000). Recently, we have demonstrated that activation of κ opioid receptors stimulates Na^+, H^+-exchanger 3 activity via Na^+, H^+-exchanger regulatory factor-1/Ezrin-radixin-moesin-binding phosphoprotein-50 independent of pertussis toxin-sensitive G proteins (Huang et al., 2004). μ, δ and κ opioid receptors have been cloned. Opioid receptors belong to the rhodopsin sub-family of the GPCR family. All GPCRs are integral membrane proteins and have seven transmembrane domains.

In the present study, we found that κ opioid receptors in human placenta membranes and FLAG-human κ opioid receptor (FLAG-hKOR) expressed in CHO cells were localized in lipid rafts. We then used CHO cells stably transfected with FLAG-hKOR cDNA, which has a signal peptide preceding the FLAG-hKOR (CHO-sFLAG-hKOR) as a model system to investigate whether disruption of lipid rafts by cholesterol reduction affected binding properties and signal transduction of the κ opioid receptor.

Materials and Methods

Materials: [^{3}H]diprenorphine (58 Ci/mmole) and [^{35}S]guanosine 5-(γ-thio)triphosphate (GTPγS) (1250 Ci/mmole) were purchased from Perkin-Elmer Co. (Boston, MA). Naloxone was a gift from the former DuPont/Merck Co. (Wilmington, DE). (-)(*trans*)-3, 4-dichloro-N-methyl-N-[2-(1-pyrrolidiny) cyclohexyl]benzeneacetamide (U50,488H) was purchased from Tocris (Ellisville, MO). Sodium carbonate, 2-morpholinoethanesulfonic acid (MES), glycerol, ethylenediamine tetraacetic acid (EDTA), ethylene glycol-bis(β-aminoethyl ether)-N,N,N',N'-tetraacetic acid (EGTA), dithiothreitol (DTT), phenylmethanesulfonyl fluoride (PMSF), leupeptin, GDP, GTPγS, methyl-β-cyclodextrin (MCD), cholesterol-methyl-β-cyclodextrin (CH-MCD) and anti-FLAG polyclonal antibody (F7425) were purchased from Sigma Co. (St Louis, MO). For phosphate assay, hydrogen peroxide, Fisk-Subbarrow reducer and phosphate standard were obtained from Sigma (St Louis, MO) and ammonium molybdate was purchased from Fisher (Newark, DE). Ammonium persulfate was purchased from Bio-Rad Laboratories (Hercules, CA). Anti-caveolin-1 monoclonal antibody (clone 2297) and anti-flotillin-1 monoclonal antibody (clone 18) were obtained from BD Transduction Laboratories (San Jose, CA). Polyclonal anti-$G_{i\alpha 3}$ antibody, which recognizes $G_{i\alpha 1}$, $G_{i\alpha 2}$ and $G_{i\alpha 3}$, and Protein A/G PLUS-Agarose were obtained from Santa Cruz Biotechnology (Santa Cruz, CA) and Immobilon-P transfer membrane from Millipore Corporation (Billerica, MA). PhosphoPlus p44/42 MAP kinase (Thr^{202}/Tyr^{204}) antibody kit and p44/42 MAP kinase antibody kit were obtained from Cell Signaling (Beverly, MA). Goat anti-mouse IgG conjugated with horseradish peroxidase (HRP) was from Jackson ImmunoResearch Laboratories, Inc. (West Grove, PA). Goat anti-rabbit IgG conjugated with HRP, SuperSignal

West Pico Chemiluminescent Substrate Solution and Restore™ Western Blot Stripping Buffer were from Pierce Co. (Rockford, IL). Pansorbin was from Calbiochem (La Jolla, CA). Complete™ Protease Inhibitor Cocktail was from Roche (Nutley, NJ).

Preparation of human placenta membranes: Fresh human placenta was obtained immediately after Cesarean section from Labor & Delivery Room of Temple University Hospital. The study qualifies as exempt under the Code of Federal Regulations and has been approval by Temple University IRB. The tissue was washed with cold 0.9% normal saline to remove as much blood as possible. The fetal side was cleared of connective tissues as much as possible and minced with scissors. The tissue was then homogenized in 10 volumes of 10 mM Tris-HCl / 1 mM EGTA / 0.32 M sucrose / 10 mM glucose / 10 μM leupeptin (pH 7.4), first with a polytron then with a Teflon pestle/glass homogenizer. After centrifugation at ~ 1000 x g for 10 min, the supernatant was saved and centrifuged again at ~40,000 x *g* for 20 min. The pellet was resuspended in buffer A (5 mM Tris-HCl, 5 mM EDTA, 5 mM EGTA and 10 μM leupeptin, pH 7.4), stayed on ice for 30 min, homogenized, and centrifuged at ~40,000 x *g* for 30 min. The pellet was saved and kept at -80°C for detergent-free lipid raft preparations. All procedures were performed at 4°C or on ice.

Detergent-free lipid rafts preparation*:* Detergent-free lipid raft preparations were conducted according to Song et al. (1996). Clonal CHO cells stably expressing FLAG-hKOR (Li et al., 2002) were detached by Versene solution (EDTA 0.54 mM, NaCl 136.9 mM, KCl 2.7 mM, Na_2HPO_4 8.1 mM, KH_2PO_4 1.46 mM, glucose 1 mM, pH 7.0) , counted by use of a Z1 Coulter Particle Counter and centrifuged at 300 x g for 2 min.

Cell pellet (~10^8 Cells) or placenta membranes (from ~6 g wet weight) was re-suspended in 2 ml of 500 mM sodium carbonate buffer (pH 11) containing 1 μM PMSF and homogenized

using a Wheaton loose fitting glass Dounce homogenizer (10 strokes) followed by sonication (three 20-s bursts) on ice using a Fisher sonicator. Two ml of 90% sucrose prepared in MES buffer (20% glycerol, 150 mM NaCl, 2 mM EDTA, 25 mM MES, pH 6.5) was added to the homogenized samples yielding 45% sucrose in a total volume of 4 ml. A discontinuous sucrose gradient was layered on the top of the 45% fraction with 4 ml of 35% sucrose and 4 ml of 5% sucrose in MES buffer containing 250mM sodium carbonate. For continuous sucrose gradients, 7 ml of 45% sucrose and 7 ml of 5% sucrose, both in MES buffer with 250mM sodium carbonate, were used to make the gradient. The homogenized samples were layered at bottom of the gradients. Isopycnic ultracentrifugation was then carried out at 40,000 rpm (200,000 x *g*) using a SW 41 rotor for 16~20 h at 4°C. Following ultracentrifugation, twelve 1-ml fractions were collected from the bottom of the gradient tube using a peristaltic pump (Rainin Co., Woburn, MA).

Determination of cholesterol and phopholipid contents: Lipids in intact cells and the twelve fractions isolated from the sucrose density gradient tube were extracted by a chloroform : methanol solvent mixture (2:1, v/v). The chloroform layer was taken out for cholesterol and phospholipid determinations. Cholesterol content was determined using cholesterol reagent obtained from Waco (cholesterol E). Briefly, upon addition of 300 µl of the color reagent, samples were incubated for 5 min at 37 °C followed by spectrophotometric analysis (absorption at 600 nm). In this reaction, cholesterol esters were hydrolyzed to free cholesterol and fatty acid in a reaction catalyzed by cholesterol oxidase and generated hydrogen peroxide. The hydrogen peroxide formed participated in the quantitative oxidative condensation between 3,5-dimethoxy-N-ethyl-N-(2-hydrixt-3-sulfopropyl)-aniline, sodium salt (DAOS) and 4-aminoantipyrine in the presence of peroxidase. The product of the reaction was a blue pigment. The total amount of

JPET Fast Forward. Published on February 27, 2006 as DOI: 10.1124/jpet.105.099507
This article has not been copyedited and formatted. The final version may differ from this version.

cholesterol in the test sample was determined by measurement of the absorbance of the blue color at 600nm using a 6-point standard curve generated with known concentrations of cholesterol. In the cholesterol depletion assay, to standardize cholesterol content, phospholipids concentrations were determined using a phosphate assay. The phospholipid concentration was determined with the method of Bartlett (1959). Data are expressed as concentration of cholesterol / concentration of phospholipid.

Ligand binding to κ opioid receptor: Binding was performed on each fraction of human placenta or CHO-sFLAG-hKOR preparations immediately after sucrose gradient centrifugation with [^{3}H]diprenorphine (1 nM) in 50 mM Tris-HCl buffer / 1 mM EGTA (pH7.4) (TE buffer) at room temperature for 1 h in duplicate according to our published procedure (Zhu et al., 1998). Nonspecific binding was defined as binding in the presence of naloxone (10 μM).

Saturation binding of [^{3}H]diprenorphine to κ opioid receptors in membranes of CHO-sFLAG-hKOR cells treated with or without 2% MCD was performed with at least six concentrations of [^{3}H]diprenorphine (ranging from 25 pM to 2 nM), and K_d and B_{max} values were determined (Huang et al., 2001). Competition inhibition by U50,488H of [^{3}H]diprenorphine (0.5 nM) binding to κ opioid receptors was performed in the absence or presence of various concentrations of U50,488H and its K_i value was determined (Zhu et al., 1997).

Treatment of CHO-sFLAG-hKOR cells with MCD or MCD followed by CH-MCD:

CHO-sFLAG-hKOR cells were incubated at 37°C for 1 h in a serum-free medium with or without MCD at indicated concentration, medium was aspirated and cells were harvested. For cholesterol repletion experiment, after MCD pretreatment, cells were then incubated for 2 h with CH-MCD in serum-free medium. Control cells were treated with vehicle for 3 h. MCD-treated cells were treated with MCD for the last 1 h.

JPET Fast Forward. Published on February 27, 2006 as DOI: 10.1124/jpet.105.099507
This article has not been copyedited and formatted. The final version may differ from this version.

[^{35}S]GTPγS Binding: Determination of [^{35}S]GTPγS binding to G proteins was carried out using a modified procedure of Zhu et al. (1997). CHO FLAG-hKOR cells were incubated with 2% MCD for 1 h at 37°C in the serum-free medium while control cells received serum-free medium alone, cells were then washed with 100 mM phosphate-buffered saline (PBS), and membranes were prepared as described previously. Membranes (10 μg protein) were incubated in reaction buffer (50 mM HEPES, 100 mM NaCl, 5 mM $MgCl_2$, 1mM EDTA) containing [^{35}S]GTPγS (100,000-150,000 dpm, 80-100 pM) and 10 μM GDP with or without U50,488H (10^{-10}-10^{-6} M) in a total volume of 0.5 ml for 60 min at 30°C. Nonspecific binding was determined in the presence of 10 μM GTPγS. Bound and free [^{35}S]GTPγS was separated by filtration with GF/B filters under reduced pressure. Radioactivity was determined by liquid scintillation counting with a counting efficiency of 95%.

Immunoblotting of FLAG-hKOR, caveolin-1 and flotillin-1 was carried out on each fraction of sucrose gradients according to our published method (Li et al., 2002). Twenty μl of 2 x Laemmli sample buffer (4% SDS, 0.1 M DTT, 20 % glycerol, 62.5 mM Tris, pH6.8) were added to each 20-μl sample, subjected to 8% sodium dodecyl sulfate – polyacrylamide gel electrophoresis (SDS-PAGE) and protein bands were transferred to immobilon-P membrane. Membranes were incubated with 5% nonfat dried milk in TBS-T solution (10 mM Tris-HCl, 159 mM NaCl, 0.1 % Tween-20, pH 7.4) for 30 min at room temperature on an orbital shaker to block nonspecific binding and then incubated with one of the following primary antibodies at 4°C overnight on an orbital shaker: rabbit anti-FLAG polyclonal antibody (1:5,000 dilution), mouse anti-caveolin-1 monoclonal antibody (1:2,000 dilution for placenta, 1:10,000 for CHO cells) or mouse anti-flotinin-1 monoclonal antibody (1:10,000 dilution for CHO cells). After three washes with TBS-T, blots were incubated with goat anti-rabbit IgG conjugated with HRP (1:10,000), or with anti-

mouse IgG conjugated with HRP (1:5,000) for 1 h at room temperature. Membranes were washed three times with TBS-T and then reacted with SuperSignal West Pico Chemiluminescence Substrate Solution. Images were captured with a FUJIFILM LAS-1000 imaging system.

p42/p44 mitogen-activated protein (MAP) kinase phosphorylation: Cells were left untreated or treated with MCD or MCD followed by CH-MCD, suspended by Versene solution and washed with PBS buffer twice. Cells were incubated in a serum-free medium for 20 min at 37°C and then treated with or without U50,488H at 37°C for 5 min. Cells were lysed with 2 x Laemmli sample buffer and subjected to 8% SDS-PAGE. Phosphorylated MAP kinase and total p44/42 MAP kinase was detected by immunoblotting as we described previously (Huang et al., 2004). The amounts of phosphorylated and total MAP kinases were quantified with the ImageGauge software. For each condition, phosphorylated MAP kinases were normalized against total MAP kinases and data were expressed as fold of stimulation over the control basal level.

Co-immunoprecipitation of the FLAG-hKOR and caveolin-1*:* CHO cells stably expressing FLAG-hKOR were treated with vehicle or 2% MCD at 37°C for 1 h and harvested. Cells were solubilized in the solubilization buffer (2% Triton X-100, 150 mM NaCl, 1 mM EDTA, 50 mM Tris HCl, pH 7.4, and Complete^{TM} Protease Inhibitor Cocktail) for 1 h at 4°C on a rocking shaker and then centrifuged at 100,000 x g for 1 h. The supernatant was incubated for 1 h at 4°C with rabbit polyclonal antibody against FLAG at 3 μg/ml or with the antibody preincubated with FLAG peptide (15 μg/ml, 30 min) as the control. Twenty μl Pansorbin was then added to precipitate the immunocomplex for 1 h at 4°C. The mixture was centrifuged and the pellets washed three times by centrifugation and resuspension. Immunoprecipitated materials were dissolved in 2 x Laemmli sample buffer, subjected to 8% SDS-PAGE. Caveolin-1 was detected

JPET Fast Forward. Published on February 27, 2006 as DOI: 10.1124/jpet.105.099507
This article has not been copyedited and formatted. The final version may differ from this version.

by western blot using a monoclonal anti-caveolin-1 (1:1,000) as described above. The membranes were then stripped at 37°C for 10 min with Restore™ Western Blot Stripping Buffer and rinsed 3 times with TBS-T and blotted with M2 mouse monoclonal antibody against FLAG followed by goat anti-mouse IgG conjugated with HRP and chemiluminescence reagents to determine the amount of FLAG-hKOR immunoprecipitated.

Co-immunoprecipitation of $G_{\alpha i}$ and caveolin-1: CHO cells stably expressing FLAG-hKOR were incubated with vehicle or 2% MCD at 37°C for 1 h and harvested. Cells were solubilized in the \solubilization buffer at 4°C for 1 h and centrifuged at 100,000 x g, 4°C for 30 min. Supernatants were collected and incubated with or without 10 µl (2 µg) of rabbit anti-$G_{\alpha i-3}$ at 4°C for 1 h, and then 20 µl of re-suspended Protein A/G PLUS-Agarose for 1 hr at 4°C on a rocker platform. The agarose pellets were collected, washed with 1.0 ml of TBS-T for 4 times, and re-suspended in 40 µl of 2 x Laemmli sample buffer. Twenty µl of each samples were separated on SDS-PAGE and caveolin-1 was detected using a monoclonal anti-caveolin-1 (1:1,000) as described above. Membranes were then stripped and $G_{\alpha i}$ proteins on the membranes were detected with immunoblotting using rabbit anti-$G_{\alpha i-3}$ (1:250), followed by goat anti-rabbit IgG conjugated with HRP and chemiluminescence reagents.

JPET Fast Forward. Published on February 27, 2006 as DOI: 10.1124/jpet.105.099507
This article has not been copyedited and formatted. The final version may differ from this version.

Results

Detergent-free lipid rafts preparation

The human placenta has a high level of κ, but not μ or δ, opioid receptors (Porthe et al., 1981; Mansson et al., 1994), which are present in brush border membranes of microvilli. Placenta membranes were sonicated and the mixture was fractionated in a 5%/35%/45% discontinuous sucrose density gradient by ultracentrifugation. From the sucrose density gradient, twelve fractions were collected. Cholesterol levels peaked in fraction 4, which was in 5% sucrose and near the interface of 5%/35% sucrose in the gradient (Fig. 1A). Caveolin-1 immunoreactivity also peaked in fraction 4 (Fig. 1C). Since low density and high levels of cholesterol and caveolins are characteristics of lipid rafts microdomains (Okamoto et al., 1998), these results validate the detergent-free lipid rafts preparation method we used. It should be noted that this method does not distinguish between planar lipid rafts and caveolae. The term lipid rafts will be used in this paper.

κ opioid receptors in the human placenta are localized in lipid rafts

Placenta membranes were subject to lipid rafts preparation procedures. The highest level (~50%) of [^{3}H]diprenorphine binding, a non-selective opioid antagonist, was detected in fraction 4 (Fig. 1B), coincided with the peaks of cholesterol and caveolin-1. The rest of binding activities spread among other fractions (Fig. 1B). Therefore, >50% of the receptor was present in fractions 1-5. These results indicate that the majority of κ opioid receptors in placenta membranes are localized in lipid rafts.

FLAG-hKOR expressed in CHO cells is localized in lipid rafts microdomains

Since the human placenta is not amenable to biochemical manipulation, we determined whether FLAG-hKOR stably expressed in CHO cells is localized in lipid rafts.

CHO cells were subject to the detergent-free lipid rafts preparation procedure as described for placenta membranes. A narrow milky band appeared in the low density region (fractions 4 and 5). High cholesterol levels were found in the fractions 1-5, with the highest level in fractions 4 or 5 (Fig. 2A), likely due to slight variations in fraction collection. The majority of [^{3}H]diprenorphine specific binding to the KOR and FLAG and caveolin-1 immunoreactivities were located in fractions 1-5, with the highest level in fraction 4 or 5 (Fig. 2C, 2D). Fig. 2 shows representative results with a peak in fraction 4. In contrast, the majority of proteins were in higher density fractions, particularly fractions 10-12 (Fig. 2B). These results indicate that the KOR in CHO cells is located in lipid raft microdomains of plasma membranes. We thus used CHO cells stably expressing FLAG-hKOR for further study.

Cholesterol reduction by MCD pretreatment and replenishment by CH-MCD

Cholesterol binding reagent MCD was used to extract cholesterol from plasma membranes of intact cells. Pretreatment of CHO-sFLAG-hKOR cells with MCD for 1 h at 37°C reduced cholesterol content in a dose-dependent manner with 0.5, 1 and 2 % MCD causing reductions of 32%, 43% and 48%, respectively (Fig. 3A). Pretreatment with 2% MCD followed by different concentrations of CH-MCD restored and then increased cell cholesterol contents in a dose-dependent manner (Fig. 3B). In the following experiments, 2% MCD was used for cholesterol reduction and 2% MCD followed by 1mg/ml CH-MCD was employed for cholesterol replenishment, unless indicated otherwise.

Effects of pretreatment with MCD or MCD/CH-MCD on cell morphology

The majority of control cells are spindle-shaped (Fig. 4A). All cells treated with 2% MCD for 1 h became spherical (Fig. 4B). Following MCD treatment, CH-MCD dose-dependently restored shape of the cells toward the control state (Fig. 4C-4E). These results indicate that cholesterol plays a key role in maintaining the morphology of CHO cells.

MCD treatment disrupted lipid rafts and shifted FLAG-hKOR and caveolin-1 to higher density fractions and the effects were reversed by CH-MCD

CHO-sFLAG-hKOR cells were left untreated or treated with 2% MCD or 2% MCD followed by 1 mg/ml CH-MCD. , and subject to detergent-free lipid rafts preparation procedures. In order to facilitate detection of the shift caused by MCD and MCD/CH-MCD treatments, we used *continuous* sucrose gradients (5% to 45%) instead of discontinuous sucrose gradients for these experiments.

In control cells, high cholesterol contents were found in fractions 1-4 with the peak at the 2nd fraction in control cells (Fig. 5A i). High levels of [^{3}H]diprenorphine binding and FLAG immunoreactivities were found in fractions 1-3 with the peak at the 2nd fraction (Fig. 5A ii, iii). Caveolin-1 was distributed in fractions 1-5 with the highest in the 2nd and 3rd fractions (Fig. 5A iii). Flotillin-1, another protein residing predominantly in lipid rafts (Bickel et al., 1997; Volonte et al., 1999), had highest levels in fractions 1-3 (Fig. 5A, iii)

In 2% MCD treated cells, cholesterol levels were greatly reduced in fractions 1-4, (Fig. 5B i), indicating that MCD treatment disrupts lipid rafts. Following MCD treatment, high levels of [^{3}H]diprenorphine binding were shifted to fractions 5-7 with the peak at the 6th fraction (Fig. 5B ii) and FLAG-hKOR immunoreactivity peaked at the 6th fraction (Fig. 5B iii). The highest levels of caveolin-1 were found in the 6th and 7th fractions (Fig. 5B iii). However, flotillin-1

JPET Fast Forward. Published on February 27, 2006 as DOI: 10.1124/jpet.105.099507
This article has not been copyedited and formatted. The final version may differ from this version.

remained in low-density fractions. Thus, FLAG-hKOR and caveolin-1 are shifted to fractions of higher density following MCD pretreatment.

In cells treated with 2% MCD followed by 1 mg/ml CH-MCD, high cholesterol contents were restored in fractions 1-4 (Fig. 5C i) with a pattern comparable to that in control cells. High levels of [^{3}H]diprenorphine binding and FLAG immunoreactivities were found in fractions 1-4 with the 3rd being highest (Fig. 5C ii, iii). Caveolin-1 was distributed in fractions 1-6 with the highest in the 3rd fraction (Fig. 5C iii). Thus, MCD treatment followed by CH-MCD restored the patterns of distribution of cholesterol, hKOR and caveolin-1, resembling those of control cells.

MCD and MCD-CH treatment appeared not to change caveolin-1 levels.

Effects of pretreatment with MCD and MCD/CH-MCD on ligand binding

As shown in Table 1, 2% MCD treatment did not significantly change K_d and B_{max} values of [^{3}H]diprenorphine binding to hKOR expressed in CHO cells. However, it did significantly reduce K_i value of U50,488H. Cholesterol repletion following MCD treatment returned the K_i value of U50,488H to the control levels.

Effect of pretreatment with MCD and MCD/CH-MCD on KOR agonist-stimulated [^{35}S]GTPγS binding and p42/p44 MAP kinase phosphorylation

Activation of κ opioid receptors stably expressed in CHO cells enhances [^{35}S]GTPγS binding to pertussis toxin-sensitive G proteins in membranes (Zhu et al., 1997), which has been used as a functional measure for G protein activation. MCD treatment greatly enhanced the E_{max} value of U50,488H (control, 358±30% of the basal level; 2% MCD, 570±10% of basal level, n = 4-5, $P < 0.05$ by Student's *t* test) without affecting its EC_{50} value (control, 5.4±1.2 nM; 2% MCD, 4.9±0.24, n=4-5) (Fig. 6A). In contrast, in cells treated with 2% MCD followed by 1 mg/ml CH-MCD, the EC_{50} (5.9±0.4 nM) and E_{max} (319 ± 14% of the basal level, n=3) values of U50,488H

JPET Fast Forward. Published on February 27, 2006 as DOI: 10.1124/jpet.105.099507
This article has not been copyedited and formatted. The final version may differ from this version.

were similar to those in control cells. Pretreatment with MCD or MCD/CH-MCD did not affect the basal [^{35}S]GTPγS binding.

The enhancement in U50,488H-induced [^{35}S]GTPγS binding following MCD pretreatment was due to an increase in the apparent B_{max} value (control, 308±12 fmole/10^7 cells, 515 ± 34 fmole/10^7 cells, n=3) of [^{35}S]GTPγS binding to Gα proteins without changing its apparent K_d value (control 1.00± 0.03 nM, MCD 1.30± 0.10 nM, n=3) (Fig. 6B).

Stimulation of κ opioid receptors has been previously demonstrated to result in enhanced p42/p44 MAP kinase phosphorylation (Li et al., 1999; Bohn et al., 2000), which is mediated by βγ subunits of pertussis-sensitive G proteins (Bohn et al., 2000). Pretreatment of cells with MCD enhanced the extent of U50,488H-promoted p42/p44 MAP kinase phosphorylation (Fig. 7). In addition, in cells pretreated with MCD/CH-MCD, U50,488H stimulated p42/p44 MAP kinase phosphorylation to similar extents as in control cells (Fig. 7).

We have performed [^{35}S]GTPγS binding using low-density CHO-sFLAG-hKOR membranes isolated with sucrose gradients. However, we were not able to detect any agonist-stimulated [^{35}S]GTPγS binding. This is likely due to the harsh condition used for preparation (0.5 M sodium carbonate buffer, pH 11) that may disrupt G protein structure and/or receptor – G protein coupling.

We have also examined effects of cholesterol reduction on U50,488H-induced inhibition of forskolin-stimulated adenylyl cyclase. However, 2% MCD pretreatment greatly reduced forskolin-stimulated adenylyl cyclase activity (data not shown), which made it difficult to assess U50,488H-induced inhibition. Varga *et al*. (1998, 1999) detected adenylyl cyclase types 6 and 7 mRNAs and type 6 protein in CHO cells. Studies have suggested that Ca^{2+}-sensitive adenylyl cyclases (particularly isoforms 5, 6 and 8) are enriched in lipid rafts, whereas Ca^{2+}-insensitive

adenylyl cyclases (isoforms 2, 4 and 7) are excluded (Crossthwaite *et al.*, 2005). It is plausible that adenylyl cyclases in CHO cells are in lipid rafts and cholesterol depletion by MCD treatment attenuates its activity.

Co-immunoprecipitation of caveolin-1 with FLAG-hKOR and effect of MCD treatment

Couet et al. (1997) found that the caveolin-1 (82-101) peptide bound to two binding motifs with the sequences of ϕXϕXXXXϕ and ϕXXXXϕXXϕ, where ϕ an aromatic residue (Trp, Phe, or Tyr). The κ opioid receptors has the ϕXϕXXXXϕ motif in the intracellular end of the seventh transmembrane helix (TM7) and the beginning of the C-terminal domain: $Y^{7.53(330)}$AFLDENF$^{7.60(337)}$. We thus examined whether the FLAG-hKOR co-immunoprecipitated with caveolin-1.

CHO-sFLAG-hKOR cells were solubilized with 2% Triton X-100 and centrifuged at 100,000 x g for 1 h. (Note: In the literature, Trition X-100 concentration used to solubilize non-lipid rafts membranes and, thus, define lipid rafts, ranged from 0.1% to 1%) (Brown and Rose, 1992). To assess whether the FLAG-hKOR was still present in low-density fractions after 2% Triton X-100 solubilization, we fractionated the 100,000 x g supernatant in a 5-45% sucrose gradient. The vast majority of FLAG-hKOR immunoreactivities were detected in the fractions 8-12 (Fig. 8A). Thus, the receptor is no longer localized in lipid rafts, indicating that the receptor is solubilized from lipid rafts. The supernatant was immunoprecipitated with FLAG antibodies. Immunoprecipitated materials were resolved on SDS-PAGE and immunoblotted with caveolin-1 antibodies. As shown in Fig. 8B, caveolin-1 immunoprecipitated with FLAG-hKOR and MCD-pretreatment did not affect co-immunoprecipitation. When the FLAG antibody was preincubated with the FLAG peptide, little FLAG-hKOR or caveolin-1 was precipitated.

Co-immunoprecipitation of caveolin-1 with $G_{\alpha i}$ proteins and effect of MCD treatment

CHO-sFLAG-hKOR cells were solubilized with 2% Triton X-100 and centrifuged at 100,000 x g for 1 h. α subunits of G_i proteins were immunoprecipitated from the supernatant with antibodies against the $G_{\alpha i}$ proteins, but not with pre-immune serum (Fig. 9). Caveolin-1 immunoprecipitated with $G_{\alpha i}$ proteins and MCD-pretreatment reduced the amount of caveolin co-immunoprecipitated with $G_{\alpha i}$ proteins (Fig. 9).

Discussion

Constitutive compartmentalization of the hKOR in lipid rafts: We have found that κ opioid receptors in human placenta and the hKOR expressed in CHO cells are localized in low-density fractions, which are enriched in cholesterol and caveolin-1, characteristics of lipid rafts microdomains. In addition, opioid receptors in rat brain membranes were found to localize in lipid rafts microdomains[1]; however, brain lipid rafts contain a low level of caveolin-1[1]. Thus, KOR is constitutively localized in lipid rafts. Since the KOR co-immunoprecipitates with caveolin-1 in CHO cells, it is likely that the KOR resides in caveolae in these cells. Caveolae were defined morphologically as flask-shaped invaginations in plasma membranes at the ultrastructural level. However, since we have no morphological evidence, we use the term "lipid rafts".

Recently, the μ opioid receptor in adult cardiac myocytes and the nociceptin / orphanin FQ receptor expressed in HEK293 cells resides were found to reside in membrane rafts independent of agonist stimulation (Butour et al., 2004; Head et al., 2005). In addition, a number of GPCRs are localized in lipid rafts, either constitutively or induced by agonists [for reviews, see (Pike, 2003; Chini and Parenti, 2004)].

Monitoring binding and immunoreactivity: In addition to receptor binding, we monitored FLAG immunoreactivity for FLAG-hKOR in each fraction derived from CHO-sFLAG-hKOR cells and found that the distribution of FLAG-hKOR immunoreactivity was similar to that of receptor binding. Since FLAG immunoreactivity is unaffected by the procedure, the presence of high % of [^{3}H]diprenorphine binding activity in lipid rafts is not due to destruction of binding activity of receptors outside of lipid rafts in the preparation procedures. We were not able to perform immunoblotting on fractions derived from placenta since to the best

of our knowledge there is no reliable antibody for immunoblotting of the κ opioid receptor. As the endogenous κ opioid receptor in the placenta is localized in lipid rafts, the localization of FLAG-hKOR in lipid rafts is not due to the signal peptide and FLAG epitope.

Effects of MCD: The direct effect of MCD on cells is extraction of cholesterol in the outer layer of plasma membranes. After cholesterol was extracted from plasma membranes, cholesterol in other intracellular compartment may efflux to plasma membranes. Since cholesterol is much more abundant in plasma membranes than in other cellular compartments, MCD effects are most significant on plasma membranes. The FLAG-hKOR construct used in the study contains a signal peptide which enhances insertion of the protein in endoplasmic reticulum membranes and thus promotes cell surface expression (Guan et al., 1992). We have found that the majority of FLAG-hKOR in CHO cells reside in plasma membranes (~75%)[2]. Thus, the MCD effects on hKOR observed from whole cell studies are likely due to its effects on plasma membranes.

Cholesterol is important for localization of the hKOR in lipid rafts, maintaining cell shape and constraining receptor – G protein coupling: Atomic force microscopy revealed that lipid rafts in model lipid bilayers were patch-like and MCD treatment resulted in reduction in size and eventual dissolution of lipid rafts in a time-dependent manner (Lawrence et al., 2003). It is conceivable that similar processes occur in plasma membranes upon cholesterol reduction and the processes are reversed during cholesterol repletion. MCD treatment shifted the KOR and caveolin-1 to medium-density fractions, changed cell shape and enhanced κ receptor mediated – G protein activation and p42/p44 MAP kinase phosphorylation. Cholesterol repletion following MCD treatment restored high cholesterol contents in low-density fractions and returned the KOR and caveolin-1 to these fractions, restored the spindle-like cell shape, and brought the signaling

back to the control levels. Taken together, these results indicate the importance of cholesterol in all these processes. In addition, MCD effects were reversed by cholesterol repletion, indicating that its effects are due to reduction in cholesterol. Since the MCD effects under the conditions used in this study were reversed by subsequent cholesterol replenishment, these results suggest that MCD does not affect cell viability.

After MCD treatment, flotillin-1 was still localized in fractions of low sucrose density. Our results are similar to those of Rajendran et al. (2003), who showed that following MCD treatment of Jurkat T cells and U937 cells, flotillin-1 remained in low density fractions. In the contrast, Urano et al. (2005) reported that flotillin-1 was shifted from low density fractions to high density fractions upon MCD treatment in human SH-SY5Y neuroblastoma cells. The reason for the differences is not clear. MCD effects on flotillin-1 location in membranes are likely cell type-dependent. Alternatively, there may be heterogeneous populations of lipid rafts, at least in some cells (Pike, 2004).

The mechanisms underlying changes in cell shape by cholesterol reduction remained to be investigated. Cholesterol depletion inhibits chemoattractant-induced neutrophil polarization and migration by abrogating prolonged activation of Rac and sustained actin polymerization (Pierini et al., 2003). Thus, cholesterol reduction may affect cytoskeleton.

Cell lines or tissues may have different cholesterol contents in membranes. Under certain physiological or pathological conditions, cholesterol contents in cells may vary. For example, synapse formation requires cholesterol delivery from astrocytes to neurons (Mauch et al., 2001). At the time of delivery, membrane cholesterol contents increased sharply. In animals having very high serum cholesterol levels, membrane cholesterol levels are likely to be increased. It is

possible that varying cholesterol contents in plasma membranes may affect opioid receptor signaling *in vivo*.

Cholesterol reduction affects hKOR – G protein signaling in CHO cells: Disruption of lipid rafts significantly enhances coupling of the hKOR to $G_{i/o}$ and cholesterol replenishment returns it to the control level. Our results are in accord with some studies in the literature, for example, those of Bari et al. (2005), Rybin et al. (2000) and Xiang et al. (2002). Bari et al. (2005) reported that in C6 glioma cells, MCD pretreatment profoundly increased CB1 cannabinoid receptor-mediated [^{35}S]GTPγS binding, p42/p44 MAP kinase phosphorylation and inhibition of forskolin-stimulated adenylate cyclase. In cardiomyocytes, cholesterol reduction augments β-adrenergic agonist-stimulated cAMP accumulation (Rybin et al., 2000) and increase in contraction rate (Xiang et al., 2002). However, in the majority of reports, cholesterol reduction results in a decrease or no change in signaling or down-stream effects mediated by GPCRs compartmentalized in lipid rafts [for a review, see (Pike, 2003) and references therein]. Effects of cholesterol reduction on GPCR signaling may depend on the receptor and cells and may be related to cholesterol contents in lipid rafts.

Possible mechanisms underlying the enhancement of κ opioid signaling by MCD treatment: The augmented agonist-induced [^{35}S]GTPγS binding is due to elevated B_{max} of [^{35}S]GTPγS binding without changing its K_d, indicating that more G proteins are activated by the hKOR. There may be two possibilities: one related to caveolin-1; the other membrane packing.

Caveolin-1: Caveolin-1 has been shown to interact, through its scaffolding domain, with many signaling molecules and inhibit signaling in most cases, including G proteins [for a review, see (Razani et al., 2002)]. Purified caveolin-1 was found to bind to purified α subunits of G_s, G_o and G_i proteins and potently inhibit activities of G_α proteins (Li et al., 1995). We have found that

caveolin-1 co-immunoprecipitates with $G_{\alpha i}$ proteins and MCD pretreatment reduced the amount of caveolin-1 co-immunoprecipitated with $G_{\alpha i}$ proteins. The reduced association, which presumably releases some inhibitory effect of caveolin-1 on the activities of $G_{\alpha i}$ proteins, results in enhanced agonist-stimulated G protein activities ([^{35}S]GTPγS binding and p42/p44 MAP kinase phosphorylation). The role of caveolins is currently being further investigated using siRNA targeting caveolins. Our findings complement those of Toselli et al. (2001), who showed that in NG108-15 cells, which lack endogenous caveolins, stable expression of caveolin-1 or -3 attenuated G proteins-mediated activities (inhibition of N-type voltage-gated Ca^{2+} channels mediated by δ opioid receptor or direct stimulation of G proteins). The observation that caveolin-1 co-immunoprecipitates with $G_{\alpha i}$ proteins is consistent with several studies, for example, De Weerd and Leeb-Lundberg (1997) and Murthy and Makhlouf (2000).

Our finding that the hKOR co-immunoprecipitated with caveolin-1 is in accord with the observations that caveolins co-immunoprecipitate with some GPCRs, for example, endothelin$_A$ (Chun et al., 1994), 5-HT$_{2A}$ (Bhatnagar et al., 2004) and μ opioid receptors (Head *et al*., 2005). MCD pretreatment did not affect co-immunoprecipitation of the hKOR with caveolin-1, indicating that enhanced receptor – G protein coupling following MCD treatment is not related to the relationship between the hKOR and caveolin-1.

Membrane packing: Cholesterol reduction by MCD significantly enhanced the affinity of U50,488H for the hKOR, which was reversed by cholesterol repletion, demonstrating that the membrane environments impact on receptor conformation. While cholesterol enrichment shifted rhodopsin and the cholecystokinin$_A$ receptor towards inactive uncoupled state, cholesterol reduction favored active conformations (Niu et al., 2002; Harikumar et al., 2005). It has been

shown that high cholesterol inhibits rhodopsin activation by reducing free volume of phospholipid acyl chain packing (Niu et al., 2002).

Sterol affects binding properties of opioid receptors: Cholesterol has been shown to modulate binding properties of opioid receptors. Here we demonstrated that cholesterol reduction by MCD enhanced the affinity of U50,488H for the hKOR, but did not affect that of [^{3}H]diprenorphine. Increasing membrane cholesterol in N1E-115 neuroblastoma cells reduced [^{3}H]met-enkephalin binding activity at the δ opioid receptor (Rao and Murphy, 1984). Sterol was reported to play roles in modulating the μ opioid receptor functions in yeast: cholesterol appeared to constrain the μ opioid receptor in an active state, while ergosterol held it in an inactive state (Lagane et al., 2000).

Lipid rafts preparation methods: Three methods and their variations have been used and each has its supporters and detractors (Pike, 2004). The first, developed by Brown and Rose (1992), involves solubilization of membranes with a non-ionic detergent such as Triton X-100 (1% at 4° C for 1 h) followed by sucrose gradient centrifugation. The second, described first by Song et al. (1996) and employed in our studies, uses sodium carbonate and brief sonication to solublize membranes followed by sucrose gradient centrifugation. The third, described by Smart et al. (1995), uses Percoll gradient to isolate plasma membranes from lysed cells, which are then sonicated followed by OptiPrep gradient centrifugation to obtain lipid rafts.

We opted not to use the detergent method for two reasons. First, we found that Triton X-100 at 0.3- 1.0% destroyed opioid receptor binding activity, which made it impossible to investigate endogenous opioid receptors in tissues and cells. Secondly, in the literature, the concentration of Triton X-100 used to obtain detergent-resistant membranes ranges from 0.1% to 1%, which may be due to the heterogeneity of lipid rafts in terms of lipid and protein

compositions in different cells / tissues (Pike, 2004). It is not certain what concentration should be used for a given tissue or cells.

Using the sodium carbonate method, we were able to detect receptor binding activity. We also showed that low-density fractions contain high levels of cholesterol in preparations from NG108-15 cells[1], rat brain[1] and rat heart, thus validating the method, in addition to CHO cells and human placenta. We routinely monitor cholesterol contents in fractions of sucrose gradient centrifugation for quality control purpose.

CHO cells as a model: Opioid receptors are distributed mainly in central and peripheral nervous systems, which have low or no caveolins (Galbiati et al., 1998). However, opioid receptors are also present in non-neuronal tissues. The κ opioid receptor is present in the human placenta (Porthe et al., 1981; Mansson et al., 1994) and the rat heart myocytes (Ventura et al., 1989; Wong et al., 1990). Caveolins are widely distributed in peripheral tissues including heart and placenta. We believe that opioid receptors expressed in CHO cells serve as a good model for opioid receptors in peripheral tissues.

In conclusion, we have found that κ opioid receptors reside in lipid rafts. Compartmentalization of the κ opioid receptor in the lipid rafts microdomain is regulated by cholesterol contents in a reversible manner and has a significant impact on κ opioid receptor-mediated G protein activation and the down-stream p42/p44 MAP kinase phosphorylation.

Acknowledgment

We thank Dr. Chad A. Grotequt of Temple University Hospital for providing human placentas.

References

Bari M, Battista N, Fezza F, Finazzi-Agro A, and Maccarrone M (2005) Lipid rafts control signaling of type-1 cannabinoid receptors in neuronal cells. Implications for anandamide-induced apoptosis. *J Biol.Chem.* **280**:12212-12220.

Bartlett GR (1959) Phosphorus assay in column chromatography. *J Biol.Chem.* **234**:466-468.

Bhatnagar A, Sheffler DJ, Kroeze WK, Compton-Toth B, and Roth BL (2004) Caveolin-1 interacts with 5-HT2A serotonin receptors and profoundly modulates the signaling of selected Galphaq-coupled protein receptors. *J Biol.Chem.* **279**:34614-34623.

Bickel PE, Scherer PE, Schnitzer JE, Oh P, Lisanti MP, and Lodish HF (1997) Flotillin and epidermal surface antigen define a new family of caveolae-associated integral membrane proteins. *J Biol.Chem.* **272**:13793-13802.

Bohn LM, Belcheva MM, and Coscia CJ (2000) Mitogenic signaling via endogenous kappa-opioid receptors in C6 glioma cells: Evidence for the involvement of protein kinase C and the mitogen-activated protein kinase signaling cascade. *J.Neurochem.* **74**:564-573.

Brown DA and Rose JK (1992) Sorting of GPI-anchored proteins to glycolipid-enriched membrane subdomains during transport to the apical cell surface. *Cell* **68**:533-544.

Butour JL, Corbani M, and Meunier JC (2004) Agonist-independent localization of the NOP receptor in detergent-resistant membrane rafts. *Biochem.Biophys.Res.Commun.* **325**:915-921.

Chini B and Parenti M (2004) G-protein coupled receptors in lipid rafts and caveolae: how, when and why do they go there? *J Mol.Endocrinol.* **32**:325-338.

Chun M, Liyanage UK, Lisanti MP, and Lodish HF (1994) Signal transduction of a G protein-coupled receptor in caveolae: colocalization of endothelin and its receptor with caveolin. *Proc.Natl.Acad.Sci.U.S.A* **91**:11728-11732.

Cohen AW, Hnasko R, Schubert W, and Lisanti MP (2004) Role of caveolae and caveolins in health and disease. *Physiol Rev.* **84**:1341-1379.

Couet J, Li S, Okamoto T, Ikezu T, and Lisanti MP (1997) Identification of peptide and protein ligands for the caveolin-scaffolding domain. Implications for the interaction of caveolin with caveolae-associated proteins. *J Biol.Chem.* **272**:6525-6533.

Crossthwaite AJ, Seebacher T, Masada N, Ciruela A, Dufraux K, Schultz JE, and Cooper DM (2005) The cytosolic domains of Ca2+-sensitive adenylyl cyclases dictate their targeting to plasma membrane lipid rafts. *J Biol Chem.* **280**:6380-6391.

De Weerd WF and Leeb-Lundberg LM (1997) Bradykinin sequesters B2 bradykinin receptors and the receptor-coupled Galpha subunits Galphaq and Galphai in caveolae in DDT1 MF-2 smooth muscle cells. *J.Biol.Chem.* **272**:17858-17866.

Galbiati F, Volonte D, Gil O, Zanazzi G, Salzer JL, Sargiacomo M, Scherer PE, Engelman JA, Schlegel A, Parenti M, Okamoto T, and Lisanti MP (1998) Expression of caveolin-1 and -2 in differentiating PC12 cells and dorsal root ganglion neurons: caveolin-2 is up-regulated in response to cell injury. *Proc.Natl.Acad.Sci.U.S.A* **95**:10257-10262.

Guan XM, Kobilka TS, and Kobilka BK (1992) Enhancement of membrane insertion and function in a type IIIb membrane protein following introduction of a cleavable signal peptide. *J.Biol.Chem.* **267**:21995-21998.

Harikumar KG, Puri V, Singh RD, Hanada K, Pagano RE, and Miller LJ (2005) Differential effects of modification of membrane cholesterol and sphingolipids on the conformation,

function, and trafficking of the G protein-coupled cholecystokinin receptor. *J Biol.Chem.* **280**:2176-2185.

Head BP, Patel HH, Roth DM, Lai NC, Niesman IR, Farquhar MG, and Insel PA (2005) G-protein-coupled receptor signaling components localize in both sarcolemmal and intracellular caveolin-3-associated microdomains in adult cardiac myocytes. *J Biol.Chem.* **280**:31036-31044.

Huang P, Kehner GB, Cowan A, and Liu-Chen L-Y (2001) Comparison of pharmacological activities of buprenorphine and norbuprenorphine: norbuprenorphine is a potent opioid agonist. *J.Pharmacol.Exp.Ther.* **297**:688-695.

Huang P, Steplock D, Weinman EJ, Hall RA, Ding Z, Li J, Wang Y, and Liu-Chen L-Y (2004) kappa Opioid receptor interacts with Na(+)/H(+)-exchanger regulatory factor-1/Ezrin-radixin-moesin-binding phosphoprotein-50 (NHERF-1/EBP50) to stimulate Na(+)/H(+) exchange independent of G(i)/G(o) proteins. *J Biol.Chem.* **279**:25002-25009.

Kilsdonk EP, Yancey PG, Stoudt GW, Bangerter FW, Johnson WJ, Phillips MC, and Rothblat GH (1995) Cellular cholesterol efflux mediated by cyclodextrins. *J Biol.Chem.* **270**:17250-17256.

Lagane B, Gaibelet G, Meilhoc E, Masson JM, Cezanne L, and Lopez A (2000) Role of sterols in modulating the human mu-opioid receptor function in Saccharomyces cerevisiae. *J Biol.Chem.* **275**:33197-33200.

Law P-Y, Wong YH, and Loh HH (2000) Molecular mechanisms and regulation of opioid receptor signaling. *Ann.Rev.Pharmacol.Toxicol.* **40**:389-430.

Lawrence JC, Saslowsky DE, Edwardson JM, and Henderson RM (2003) Real-time analysis of the effects of cholesterol on lipid raft behavior using atomic force microscopy. *Biophys.J* **84**:1827-1832.

Li J, Li J-G, Chen C, Zhang F, and Liu-Chen L-Y (2002) Molecular basis of differences in (-)(trans)-3,4-dichloro-N-methyl-N-[2-(1-pyrrolidiny)-cyclohexyl]benzeneacetamide-induced desensitization and phosphorylation between human and rat κ-opioid receptors expressed in Chinese hamster ovary cells. *Mol.Pharmacol.* **61**:73-84.

Li J-G, Luo LY, Krupnick JG, Benovic JL, and Liu-Chen L-Y (1999) U50,488H-induced internalization of the human kappa opioid receptor involves a beta-arrestin- and dynamin-dependent mechanism. Kappa receptor internalization is not required for mitogen-activated protein kinase activation. *J.Biol.Chem.* **274**:12087-12094.

Li S, Okamoto T, Chun M, Sargiacomo M, Casanova JE, Hansen SH, Nishimoto I, and Lisanti MP (1995) Evidence for a regulated interaction between heterotrimeric G proteins and caveolin. *J Biol.Chem.* **270**:15693-15701.

Li S, Song KS, and Lisanti MP (1996) Expression and characterization of recombinant caveolin. Purification by polyhistidine tagging and cholesterol-dependent incorporation into defined lipid membranes. *J Biol.Chem.* **271**:568-573.

Liu-Chen L-Y (2004) Agonist-induced regulation and trafficking of kappa opioid receptors. *Life Sci.* **75**:511-536.

Mansson E, Bare L, and Yang D (1994) Isolation of a human κ opioid receptor cDNA from placenta. *Biochem.Biophys.Res.Comm.* **202**:1431-1437.

Mauch DH, Nagler K, Schumacher S, Goritz C, Muller EC, Otto A, and Pfrieger FW (2001) CNS synaptogenesis promoted by glia-derived cholesterol. *Science* **294**:1354-1357.

Murata M, Peranen J, Schreiner R, Wieland F, Kurzchalia TV, and Simons K (1995) VIP21/caveolin is a cholesterol-binding protein. *Proc.Natl.Acad.Sci.U.S.A* **92**:10339-10343.

Murthy KS and Makhlouf GM (2000) Heterologous desensitization mediated by G protein-specific binding to caveolin. *J Biol.Chem.* **275**:30211-30219.

Niu SL, Mitchell DC, and Litman BJ (2002) Manipulation of cholesterol levels in rod disk membranes by methyl-beta-cyclodextrin: effects on receptor activation. *J Biol.Chem.* **277**:20139-20145.

Okamoto T, Schlegel A, Scherer PE, and Lisanti MP (1998) Caveolins, a family of scaffolding proteins for organizing "preassembled signaling complexes" at the plasma membrane. *J Biol.Chem.* **273**:5419-5422.

Peart JN, Gross ER, and Gross GJ (2005) Opioid-induced preconditioning: recent advances and future perspectives. *Vascul.Pharmacol* **42**:211-218.

Petit A, Gallo-Payet N, Lehoux JG, Bellabarba D, and Belisle S (1991) Adenosine 3':5'-cyclic monophosphate (cAMP) is not the mediator of kappa opiate effect on human placental lactogen release. *Life Sci.* **49**:465-472.

Pierini LM, Eddy RJ, Fuortes M, Seveau S, Casulo C, and Maxfield FR (2003) Membrane lipid organization is critical for human neutrophil polarization. *J Biol.Chem.* **278**:10831-10841.

Pike LJ (2003) Lipid rafts: bringing order to chaos. *J.Lipid Res.* **44**:655-667.

Pike LJ (2004) Lipid rafts: heterogeneity on the high seas. *Biochem.J* **378**:281-292.

Porthe G, Valette A, and Cros J (1981) Kappa opiate binding sites in human placenta. *Biochem.Biophys.Res.Commun.* **101**:1-6.

Rajendran L, Masilamani M, Solomon S, Tikkanen R, Stuermer CA, Plattner H, and Illges H (2003) Asymmetric localization of flotillins/reggies in preassembled platforms confers inherent polarity to hematopoietic cells. *Proc.Natl.Acad.Sci.U.S.A* **100**:8241-8246.

Rao BG and Murphy MG (1984) Opiate peptide receptors on intact NIE-115 neuroblastoma: radioligand binding properties, intracellular response, and effects of increasing membrane cholesterol. *Prog.Neuropsychopharmacol.Biol.Psychiatry* **8**:719-723.

Razani B, Woodman SE, and Lisanti MP (2002) Caveolae: from cell biology to animal physiology. *Pharmacol Rev.* **54**:431-467.

Roth BL, Baner K, Westkaemper R, Siebert D, Rice KC, Steinberg S, Ernsberger P, and Rothman RB (2002) Salvinorin A: a potent naturally occurring nonnitrogenous kappa opioid selective agonist. *Proc.Natl.Acad.Sci.U.S.A.* **99**:11934-11939.

Rothberg KG, Heuser JE, Donzell WC, Ying YS, Glenney JR, and Anderson RG (1992) Caveolin, a protein component of caveolae membrane coats. *Cell* **68**:673-682.

Rybin VO, Xu X, Lisanti MP, and Steinberg SF (2000) Differential targeting of beta -adrenergic receptor subtypes and adenylyl cyclase to cardiomyocyte caveolae. A mechanism to functionally regulate the cAMP signaling pathway. *J Biol.Chem.* **275**:41447-41457.

Smart EJ, Ying YS, Mineo C, and Anderson RG (1995) A detergent-free method for purifying caveolae membrane from tissue culture cells. *Proc.Natl.Acad.Sci.U.S.A* **92**:10104-10108.

Song KS, Li S, Okamoto T, Quilliam LA, Sargiacomo M, and Lisanti MP (1996) Co-purification and direct interaction of Ras with caveolin, an integral membrane protein of caveolae microdomains. Detergent-free purification of caveolae microdomains. *J Biol.Chem.* **271**:9690-9697.

Toselli M, Taglietti V, Parente V, Flati S, Pavan A, Guzzi F, and Parenti M (2001) Attenuation of G protein-mediated inhibition of N-type calcium currents by expression of caveolins in mammalian NG108-15 cells. *J Physiol* **536**:361-373.

Urano Y, Hayashi I, Isoo N, Reid PC, Shibasaki Y, Noguchi N, Tomita T, Iwatsubo T, Hamakubo T, and Kodama T (2005) Association of active gamma-secretase complex with lipid rafts. *J Lipid Res.* **46**:904-912.

Valette A, Tafani M, Porthe G, Pontonnier G, and Cros J (1983) Placental kappa binding site : interaction with dynorphin and its possible implication in hCG secretion. *Life Sci.* **33 Suppl 1**:523-526.

Varga EV, Stropova D, Rubenzik M, Waite S, Roeske WR, and Yamamura HI (1999) Phosphorylation of adenylyl cyclase VI upon chronic delta-opioid receptor stimulation. *Eur.J Pharmacol* **364**:R1-R3.

Varga EV, Stropova D, Rubenzik M, Wang M, Landsman RS, Roeske WR, and Yamamura HI (1998) Identification of adenylyl cyclase isoenzymes in CHO and B82 cells. *Eur.J Pharmacol* **348**:R1-R2.

Ventura C, Bastagli L, Bernardi P, Caldarera CM, and Guarnieri C (1989) Opioid receptors in rat cardiac sarcolemma: effect of phenylephrine and isoproterenol. *Biochim.Biophys.Acta* **987**:69-74.

Volonte D, Galbiati F, Li S, Nishiyama K, Okamoto T, and Lisanti MP (1999) Flotillins/cavatellins are differentially expressed in cells and tissues and form a hetero-oligomeric complex with caveolins in vivo. Characterization and epitope-mapping of a novel flotillin-1 monoclonal antibody probe. *J Biol.Chem.* **274**:12702-12709.

Wong TM, Lee AY, and Tai KK (1990) Effects of drugs interacting with opioid receptors during normal perfusion or ischemia and reperfusion in the isolated rat heart--an attempt to identify cardiac opioid receptor subtype(s) involved in arrhythmogenesis. *J.Mol.Cell Cardiol.* **22**:1167-1175.

Xiang Y, Rybin VO, Steinberg SF, and Kobilka B (2002) Caveolar localization dictates physiologic signaling of beta 2-adrenoceptors in neonatal cardiac myocytes. *J Biol.Chem.* **277**:34280-34286.

Zhu J, Luo LY, Mao GF, Ashby B, and Liu-Chen L-Y (1998) Agonist-induced desensitization and down-regulation of the human kappa opioid receptor expressed in CHO cells. *J.Pharmacol.Exp.Ther.* **285**:28-36.

Zhu J, Luo L-Y, Chen C, and Liu-Chen L-Y (1997) Activation of the cloned human κ opioid receptor by agonists enhances [^{35}S]GTPγS binding to membranes: Determination of potencies and efficacies of ligands. *J.Pharmacol.Exp.Ther.* **282**:676-684.

Footnotes

[1] Huang, P, Xu, W., Yoon, S. I., Chong, P. L.-G. and Liu-Chen, L. Y.: Localization of the Delta Opioid Receptor in Lipid Rafts: Effect of Agonist and Cholesterol Reduction (in preparation).

[2]Xu, W. and Liu-Chen, L. Y., unpublished observations.

This work was supported by NIH grants DA04745, DA11263 and DA17302 and supported in part by Pennsylvania Department of Health. S.-I. Y. and P.L.-G.C. acknowledge the support from AHA (0255082N) and ACS (PRF-38205-AC-7).

JPET Fast Forward. Published on February 27, 2006 as DOI: 10.1124/jpet.105.099507
This article has not been copyedited and formatted. The final version may differ from this version.

Figure Legends

Fig. 1. κ opioid receptors in the human placenta are localized in lipid rafts. Human placenta membranes were sonicated in 500 mM sodium carbonate buffer (pH 11) and then fractionated through a discontinuous sucrose gradient (5%/35%/45%) as described under Materials and Methods. Twelve fractions were collected and each fraction was subjected to

(A) Determination of cholesterol contents. Data are expressed as the ratios of [cholesterol in each fraction]/ [total phospholipids].

(B) [^{3}H]diprenorphine (~1nM) binding using naloxone (10 μM) to define nonspecific binding. Data are expressed as % of total specific [^{3}H]diprenorphine binding. In this experiment, 6 g (wet weight) of human placenta was used and 100 μl/ 1-ml fraction was used in binding in duplicate. [^{3}H]diprenorphine specific binding in the fraction 4 was 22,464 dpm/100 μl.

(C) Immunoblotting of caveolin-1 with anti-caveolin-1 monoclonal antibody.

Fig. 1 (A) and (B) represent mean ± s.e.m. of the three experiments performed with similar results. Fig. 1(C) represents one of the three experiments performed with similar results.

Fig. 2. FLAG-hKOR expressed in CHO cells is localized in low-density membrane microdomains as caveolin-1. CHO cells stably expressing FLAG-hKOR were subjected to detergent-free lipid raft preparation using 500 mM sodium carbonate buffer (pH 11) and sonication. Cells were then fractionated through a discontinuous sucrose gradient (5%/35%/45%). Twelve 1-ml fractions were collected and each fraction was examined for

(A) Determination of cholesterol contents. Data are expressed as the ratios of [cholesterol in each fraction]/ [total phospholipids].

(B) SDS-PAGE, transfer to membranes and protein staining with Ponceau S.

(C) [^{3}H]diprenorphine (~1 nM) binding using naloxone (10 μM) to define nonspecific binding. Data are expressed as % of the sum of specific [^{3}H]diprenorphine binding for each fraction. In this experiment, 1.09 x 10^8 cells were used and 100 μl out of 1-ml fraction was used in binding experiments in duplicate. The counts of [^{3}H]diprenorphine specific binding in the fraction 4 was 5,626 dpm/100 μl .

(D) Immunoblotting of FLAG-hKOR and caveolin-1 with polyclonal anti-FLAG antibody and anti-caveolin-1 monoclonal antibody, respectively. Unfractionated cells were used as the control. The figures are the representative results of the three experiments performed with similar results.

Fig. 3. Effects of pre-treatments with MCD and MCD followed by CH-MCD on cholesterol contents. CHO-sFLAG-hKOR cells were incubated at 37°C in a serum-free medium with MCD for 1 h and medium was aspirated. Cells were then incubated for 2 h with CH-MCD in serum-free medium. Control cells were treated with vehicle for 3 h. MCD-treated cells were treated with MCD for the last 1 h. [Cholesterol] / [phospholipids] ratios in cells were determined. The results represent mean ± s.e.m of the four experiments performed with similar results.

Fig. 4. Effects of treatment with MCD and MCD followed by CH-MCD on cell morphology. CHO cells stably transfected with FLAG-hKOR were treated as described in Fig. 4 legend with (A) vehicle (serum-free medium), (B) 2% MCD or (C-E) 2% MCD then 0.1, 0.5 and 1 mg/ml CH-MCD. The figures are the representative images of CHO cells.

JPET Fast Forward. Published on February 27, 2006 as DOI: 10.1124/jpet.105.099507
This article has not been copyedited and formatted. The final version may differ from this version.

Fig. 5. Effects of cholesterol reduction and repletion on lipid rafts and distribution of FLAG-hKOR and caveolin-1. CHO cells stably transfected with FLAG-hKOR were treated as described in Fig. 4 legend with 2% MCD or 2% MCD then 1 mg/ml CH-MCD. Cells were subjected to detergent-free lipid rafts preparation with centrifugation through a 5%-45% continuous sucrose gradient. Fractions were collected and examined for (i) [Cholesterol] / [phospholipids] ratios, (ii) [^{3}H]diprenorphine (~1 nM) binding, (iii) immunoblotting of FLAG-hKOR, caveolin-1 and flotillin-1.

(A) Control cells; (B) MCD-pretreated cells; (C) 2% MCD followed by 1 mg/ml CH-MCD.

(ii) Data are expressed as % of total specific [^{3}H]diprenorphine binding. Fig. 5A (i) and (ii), Fig. 5B (i) and (ii) and Fig. 5C (i) and (ii) are shown as mean ± s.e.m. of three independent experiments. Fig. 5A (iii), Fig 5B (iii) and Fig. 5C (iii) represent one of the three experiments performed with similar results.

Fig. 6. Effects of cholesterol reduction and repletion on U50,488H-stimulated [^{35}S]GTPγS binding.

(A) CHO cells stably transfected with FLAG-hKOR were treated with vehicle, 2% MCD or 2% MCD then 1 mg/ml CH-MCD. Membranes were prepared and U50,488H-stimulated [^{35}S]GTPγS binding to membranes was carried out with different concentrations. Non-specific binding determined in the presence of 10 μM cold GTPγS. Data were calculated as percentage of the basal [^{35}S]GTPγS binding. Pretreatment with MCD or MCD then CH-MCD did not affect basal binding. Data were shown as the means ± s.e.m. from three or four experiments.

(B) Displacement of [^{35}S]GTPγS binding with indicated concentrations of unlabeled GTPγS was performed in the presence and absence of 1 μM U50,488H. The data represent the differences

between stimulated and basal levels in control and 2% MCD-treated cells. The figure represents one of the three experiments performed with similar results.

Fig. 7. Effects of cholesterol reduction and repletion on U50,488H-stimulated phosphorylation of p42/p44 mitogen-activated protein kinase. CHO-sFLAG-hKOR cells were left untreated or incubated with 2% MCD or 2% MCD then 1 mg/ml CH-MCD. Cells were incubated in a serum-free medium for 20 min at 37°C and then treated with or without U50,488H at 37°C for 5 min. Phosphorylated and total p44/42 MAP kinases were detected by immunoblotting and quantitated.

(A) The figure represents one of the five experiments.

(B) Data are shown as mean ± s.e.m. of at least five independent experiments.

*$P < 0.05$, when compared with the control samples at the same concentration of U50,488H, one-way ANOVA followed by Dunnett's multiple comparison test.

Fig. 8. (A) Solubilization of FLAG-hKOR by 2% Triton X-100. CHO-sFLAG-hKOR cells were lysed, solubilized with 2% Triton X-100 at 4°C for 1 h and centrifuged at 100,000 x g for 1 h. The supernatant was separated on a continuous 5-45% sucrose gradient and twelve fractions were subject to SDS-PAGE and immunoblotted for FLAG- hKOR using FLAG antibodies.

(B) Co-immunoprecipitation of FLAG-hKOR and caveiolin-1 and effect of MCD treatment. CHO-sFLAG-hKOR cells were left untreated or treated with 2% MCD at 37°C for 1 h and harvested. Cells were solubilized and then centrifuged. The supernatant was incubated with rabbit polyclonal antibody against FLAG or with antibody preincubated with FLAG peptide followed by Pansorbin. Immunoprecipitated materials were resolved in 8% SDS-PAGE and

immunoblotting was performed with a monoclonal antibody against caveolin-1 (top). The membranes were then stripped and blotted with a mouse monoclonal antibody M2 against FLAG (bottom) for immunoprecipitated FLAG-hKOR. The figure represents one of the three experiments performed.

Fig. 9. Co-immunoprecipitation of $G_{\alpha i}$ proteins and caveiolin-1 and effect of MCD treatment. CHO-sFLAG-hKOR cells were left untreated or treated with 2% MCD at 37°C for 1 h and harvested. Cells were solubilized and then centrifuged. The supernatant was incubated with or without rabbit anti-$G_{\alpha i-3}$ antibody and then Protein A/G PLUS-Agarose. Immunoprecipitated materials were resolved in 8% SDS-PAGE and immunoblotting was performed with a monoclonal antibody against caveolin-1 (top). The membranes were then stripped and blotted again with rabbit anti-$G_{\alpha i-3}$ antibody (bottom) for immunoprecipitated $G_{\alpha i}$ proteins. The figure represents one of the three experiments performed.

JPET Fast Forward. Published on February 27, 2006 as DOI: 10.1124/jpet.105.099507
This article has not been copyedited and formatted. The final version may differ from this version.

Table 1. **Effects of MCD and MCD/CH-MCD pretreatment on K_d and B_{max} values of [^{3}H]diprenorphine binding and K_i value of U50,488H binding to FLAG-hKOR stably expressed in CHO cells**. CHO cells stably transfected with FLAG-hKOR were incubated with or without 2% MCD in a serum-free medium for 1 h at 37°C, washed and membranes were prepared. Saturation binding of [^{3}H]diprenorphine to FLAG-hKOR was performed and K_d and B_{max} values were calculated. Competition inhibition by U50,488H of [^{3}H]diprenorphine binding was conducted and its K_i value was determined. Each value represents mean ± s.e.m. of three to five experiments performed in duplicate.

	[^{3}H]diprenorphine		U50,488H
	K_d (nM)	B_{max} (fmole/10^7cells)	K_i (nM)
Control	0.14±0.02	312.9± 9.2	1.30±0.10
2% MCD	0.13±0.01	342.8±18.9	0.41±0.01**
MCD + CH-MCD	0.19±0.04	327.4±13.9	1.19±0.12

***P* <0.01, compared with the control as determined by Student's *t* test.

JPET Fast Forward. Published on February 27, 2006 as DOI: 10.1124/jpet.105.099507
This article has not been copyedited and formatted. The final version may differ from this version.

Fig. 1

A.

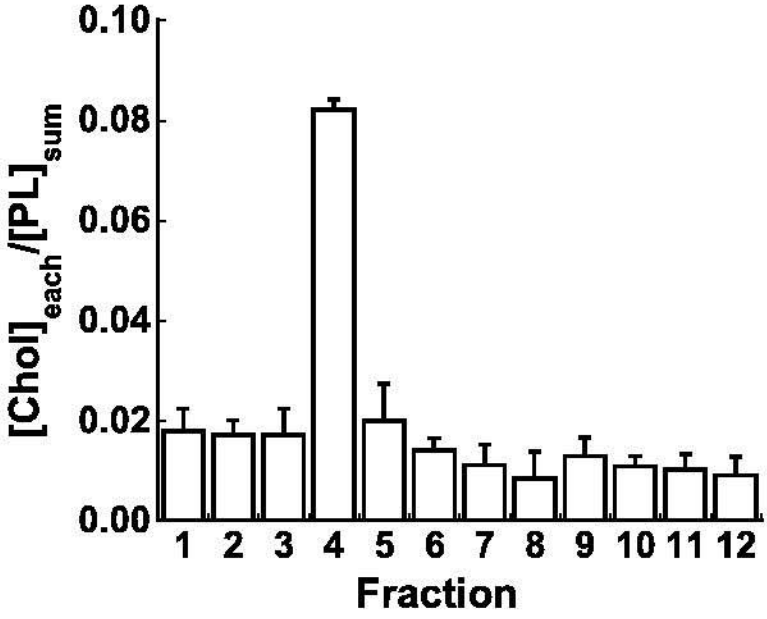

B.

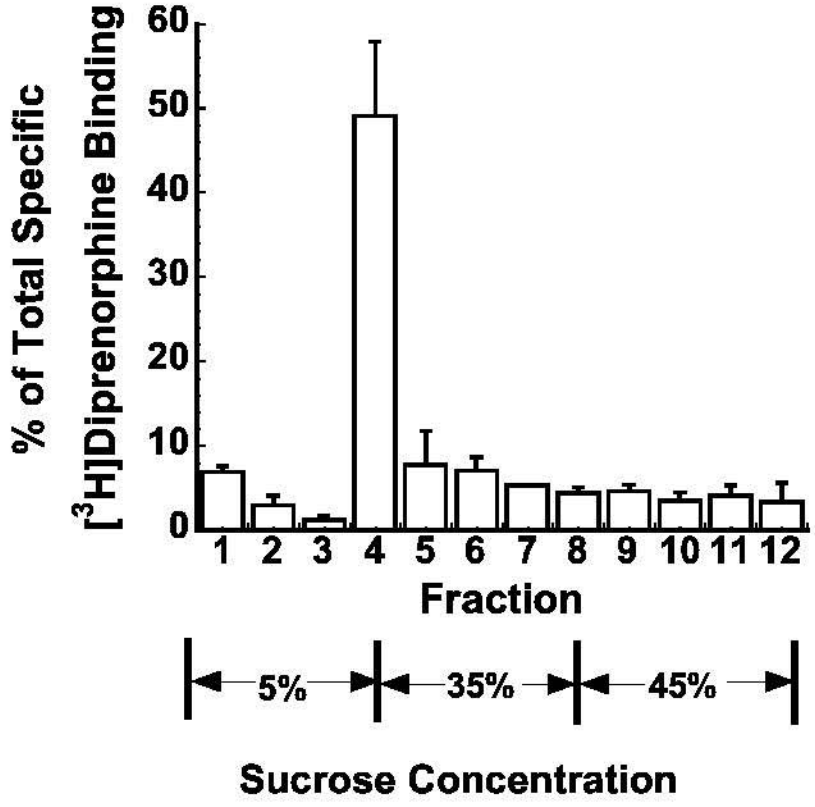

C.

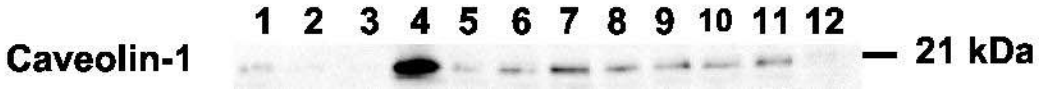

JPET Fast Forward. Published on February 27, 2006 as DOI: 10.1124/jpet.105.099507
This article has not been copyedited and formatted. The final version may differ from this version.

Fig. 2

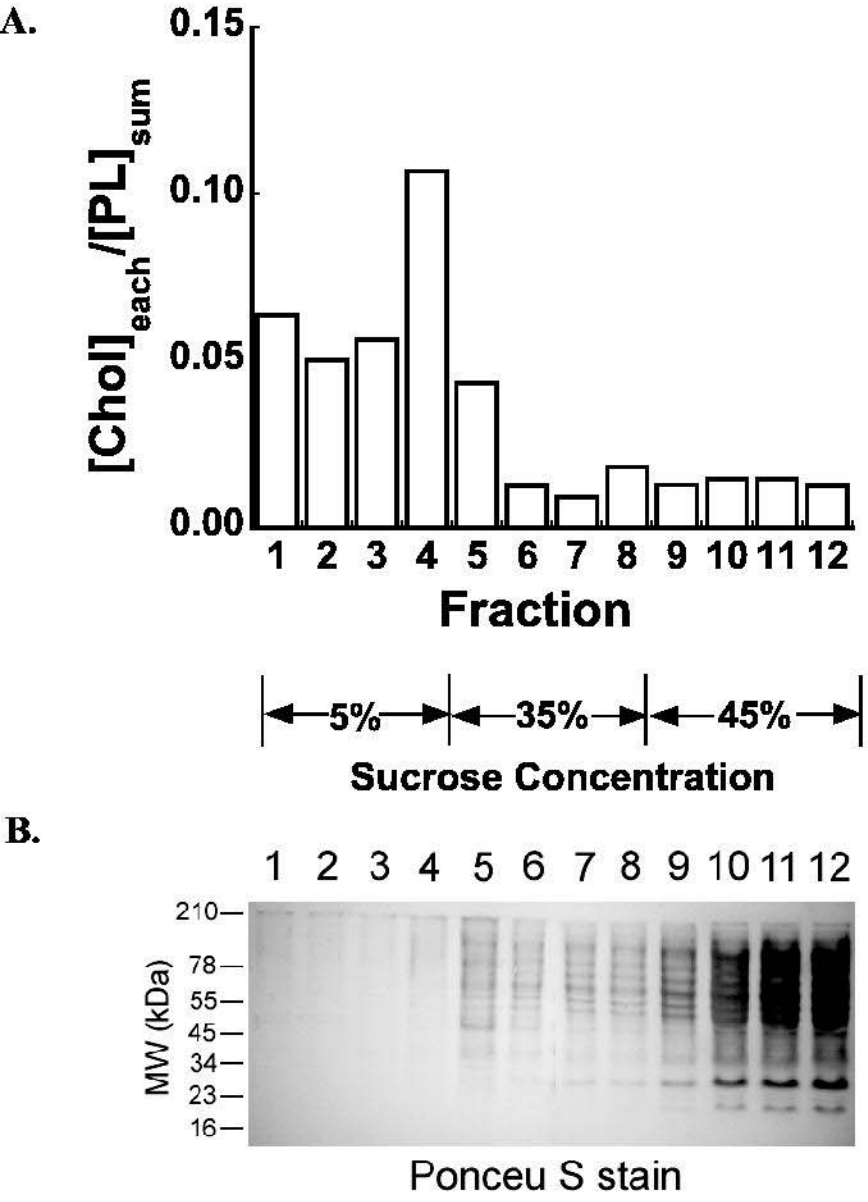

JPET Fast Forward. Published on February 27, 2006 as DOI: 10.1124/jpet.105.099507
This article has not been copyedited and formatted. The final version may differ from this version.

Fig. 2

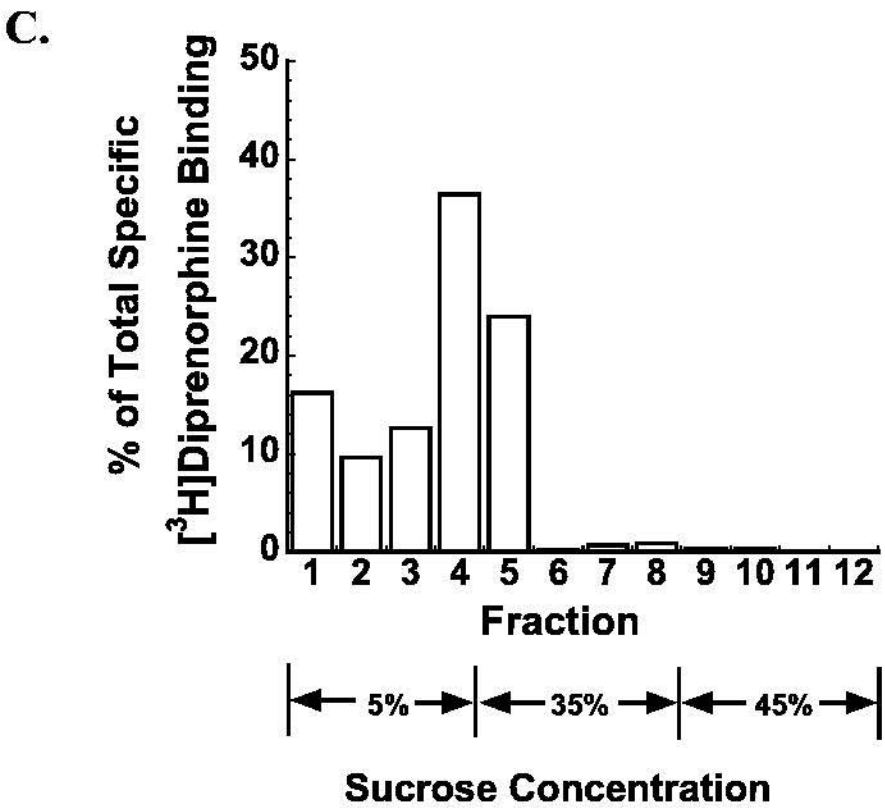

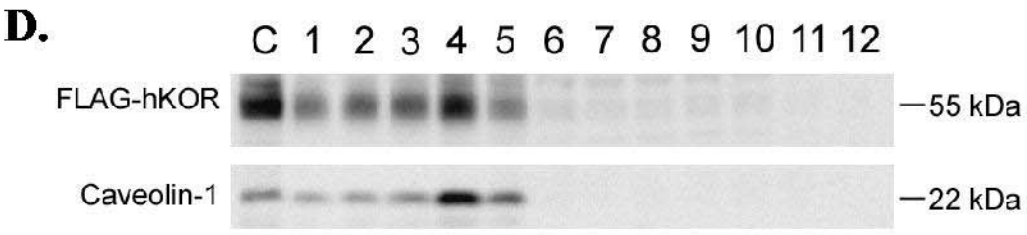

JPET Fast Forward. Published on February 27, 2006 as DOI: 10.1124/jpet.105.099507
This article has not been copyedited and formatted. The final version may differ from this version.

Fig. 3

A.

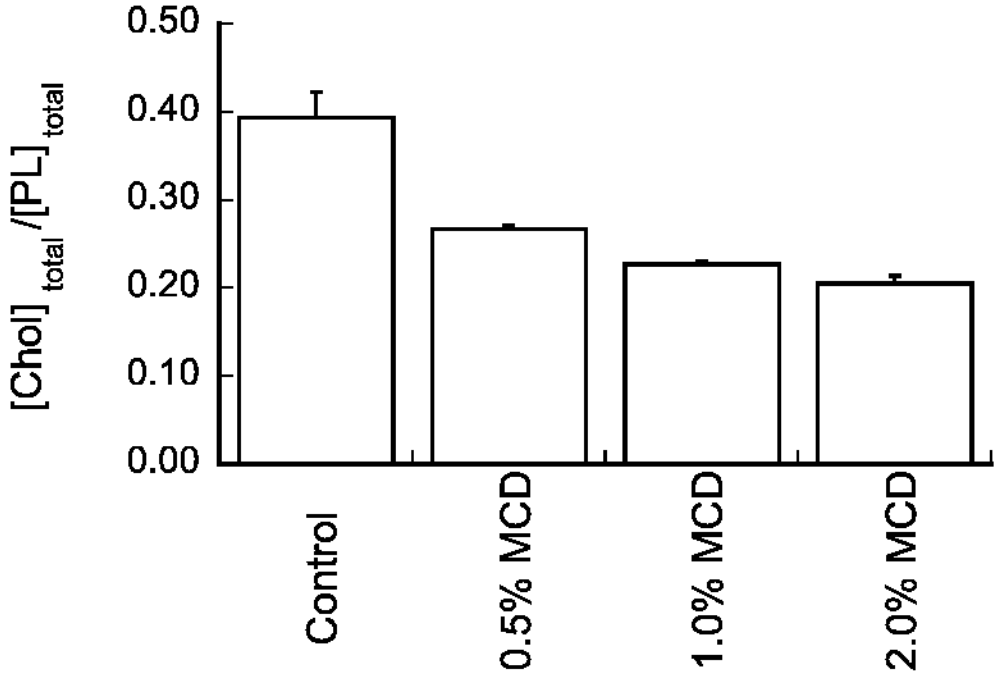

B.

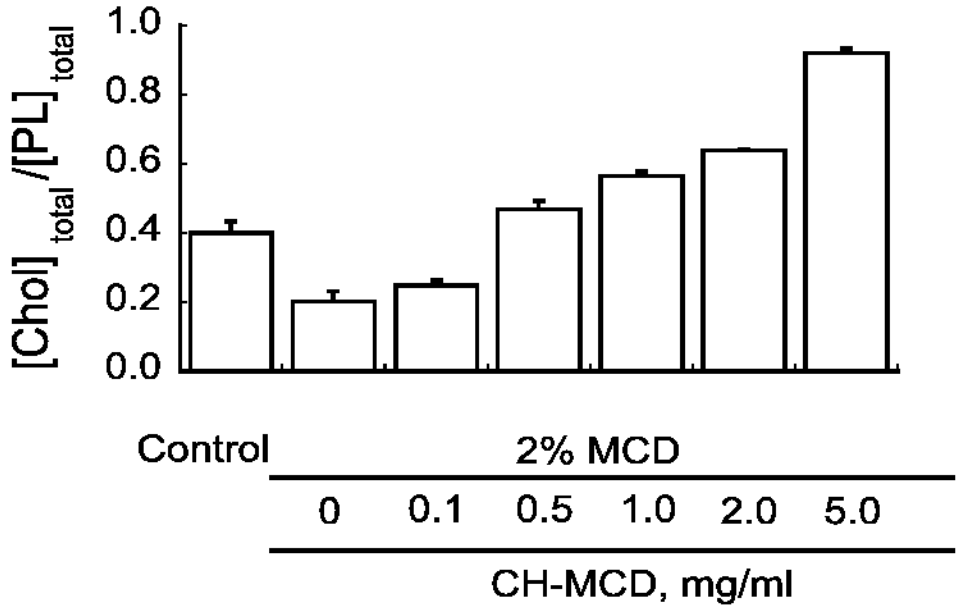

JPET Fast Forward. Published on February 27, 2006 as DOI: 10.1124/jpet.105.099507
This article has not been copyedited and formatted. The final version may differ from this version.

Fig. 4

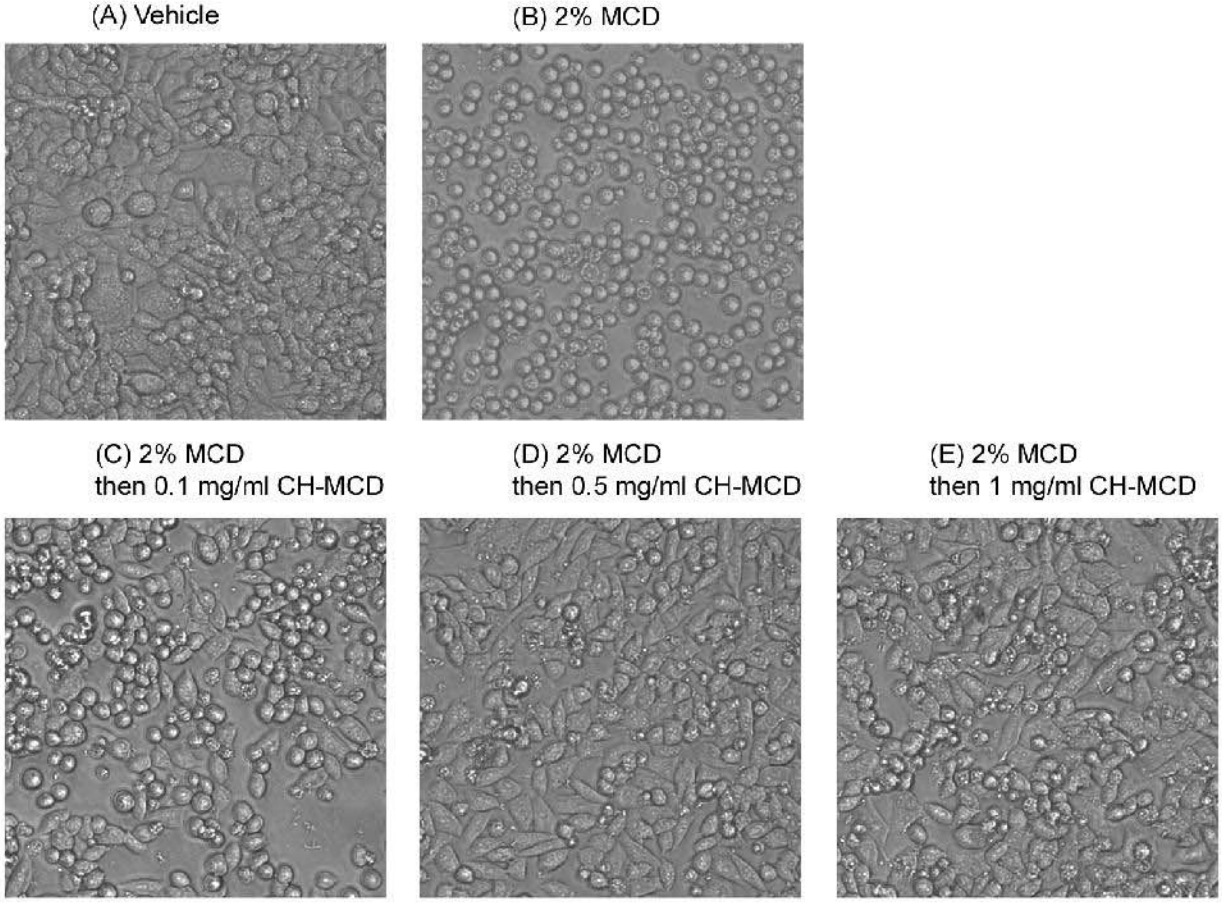

JPET Fast Forward. Published on February 27, 2006 as DOI: 10.1124/jpet.105.099507
This article has not been copyedited and formatted. The final version may differ from this version.

Fig. 5A. Control cells

(i)

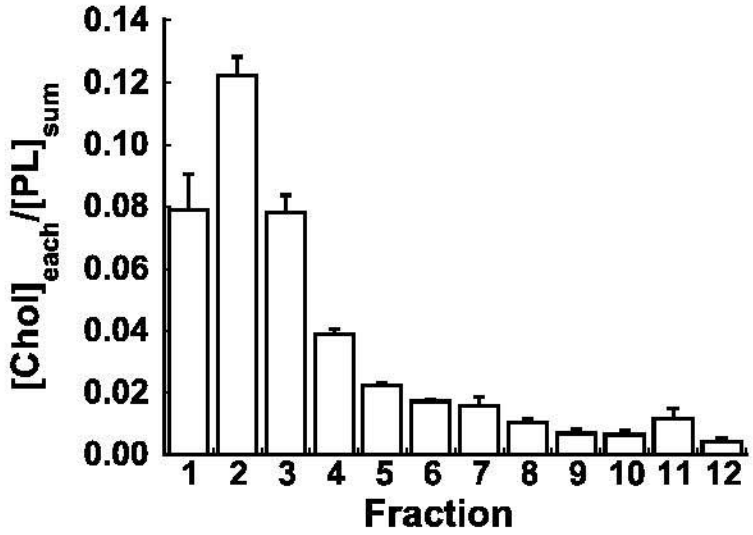

(ii)

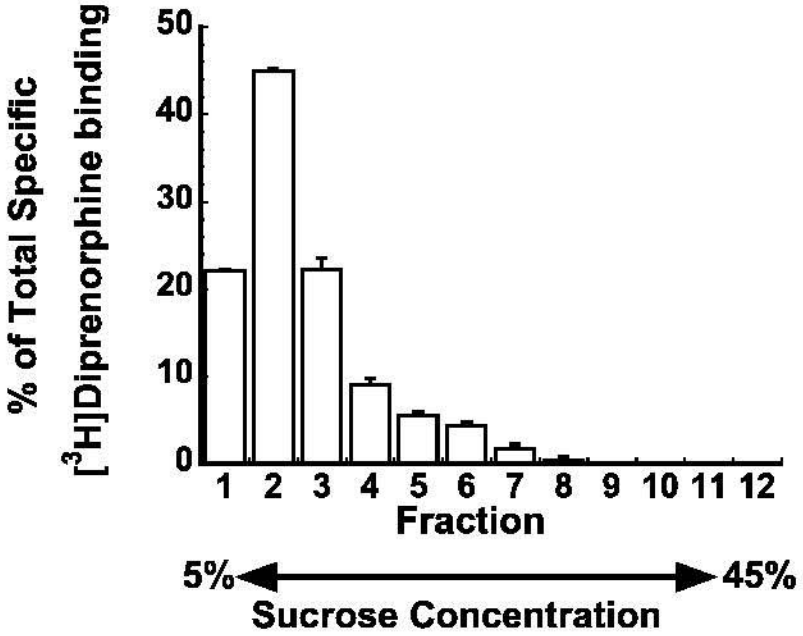

(iii)

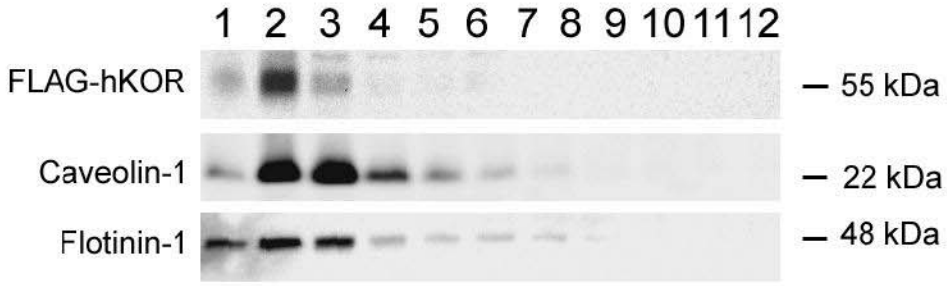

JPET Fast Forward. Published on February 27, 2006 as DOI: 10.1124/jpet.105.099507
This article has not been copyedited and formatted. The final version may differ from this version.

Fig. 5B. MCD-pretreated cells

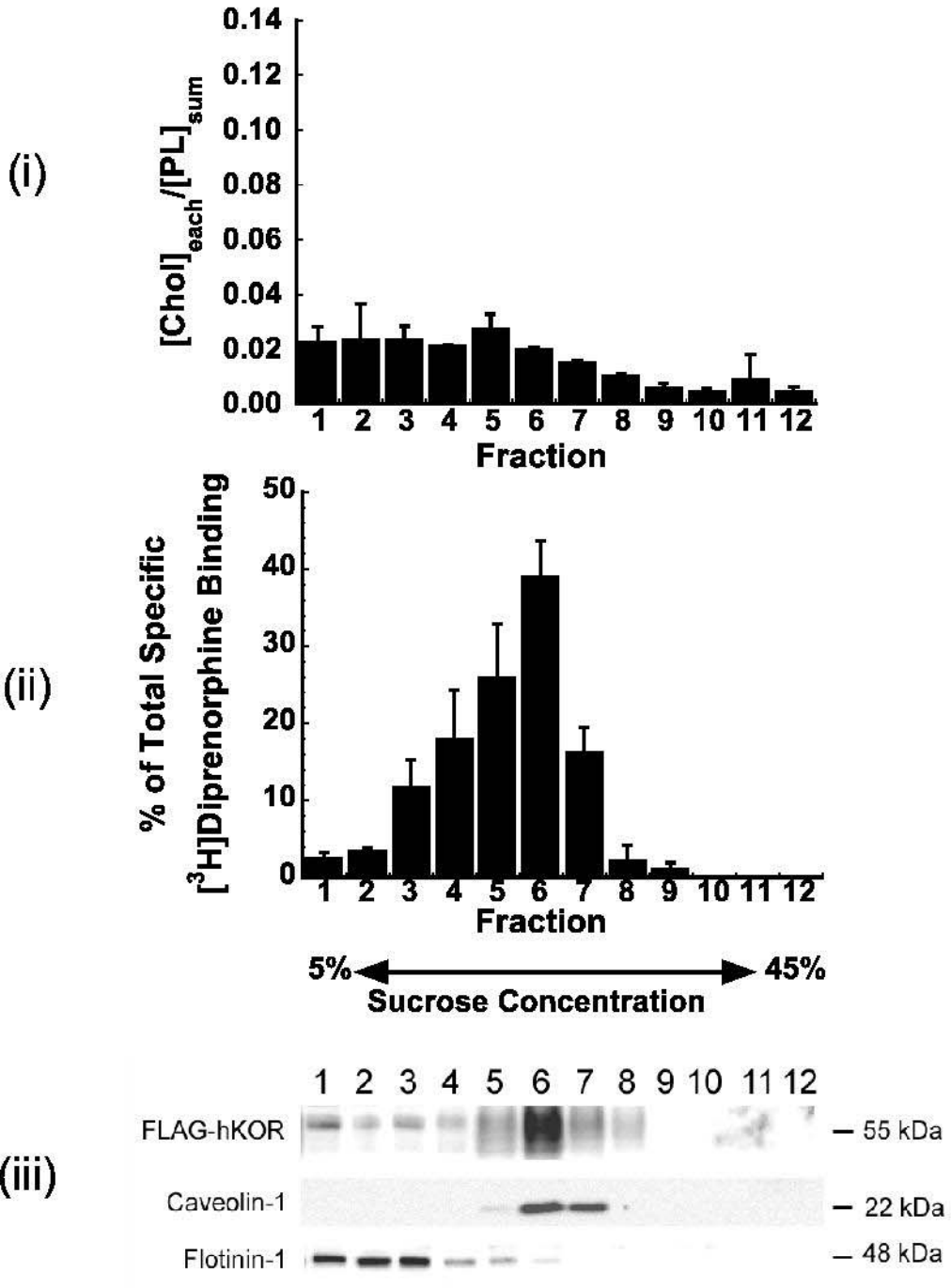

JPET Fast Forward. Published on February 27, 2006 as DOI: 10.1124/jpet.105.099507
This article has not been copyedited and formatted. The final version may differ from this version.

Fig. 5C. 2% MCD followed by 1mg/ml CH-MCD

(i)

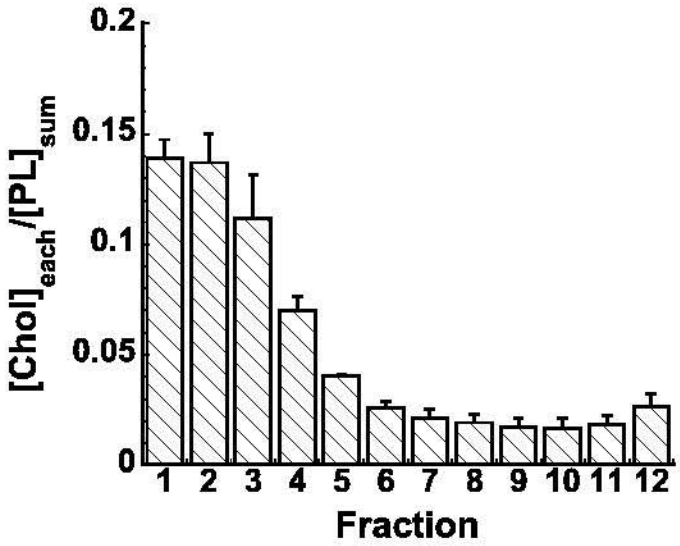

(ii)

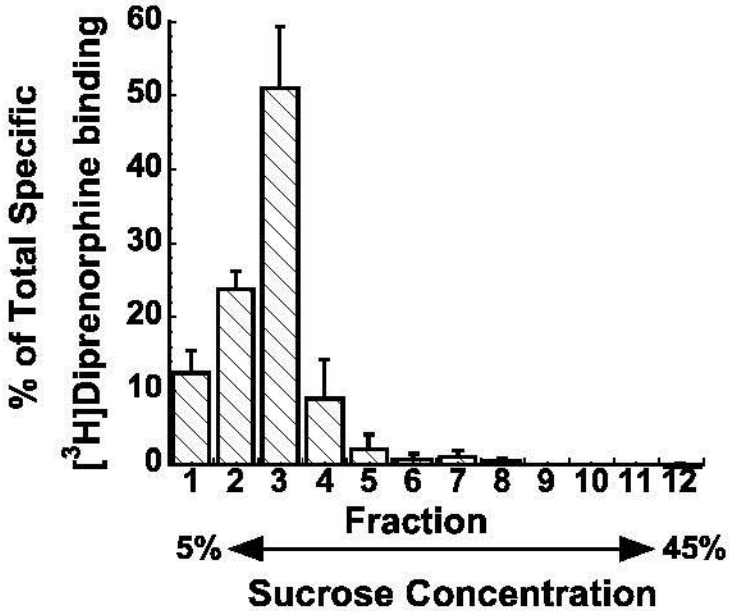

(iii)

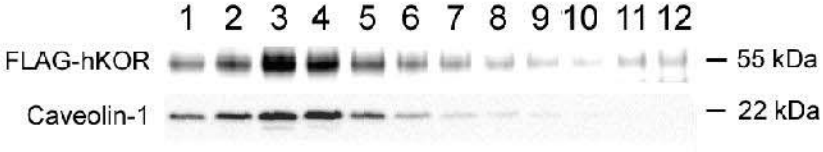

JPET Fast Forward. Published on February 27, 2006 as DOI: 10.1124/jpet.105.099507
This article has not been copyedited and formatted. The final version may differ from this version.

Fig. 6A

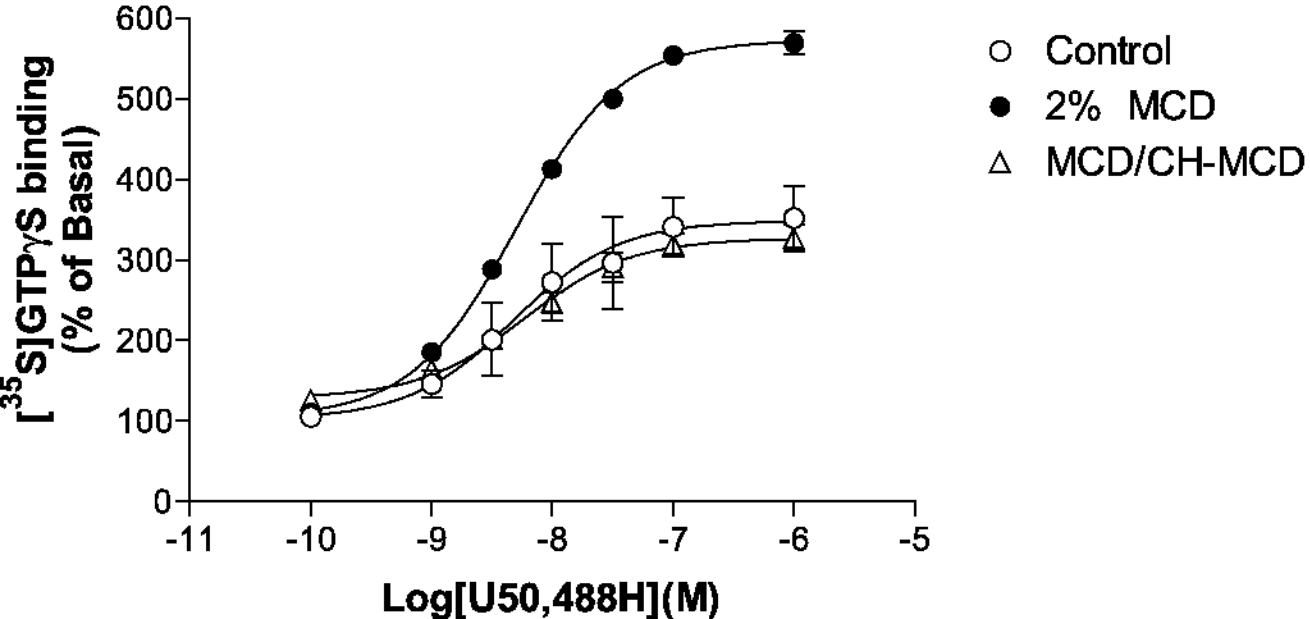

JPET Fast Forward. Published on February 27, 2006 as DOI: 10.1124/jpet.105.099507
This article has not been copyedited and formatted. The final version may differ from this version.

Fig. 6B

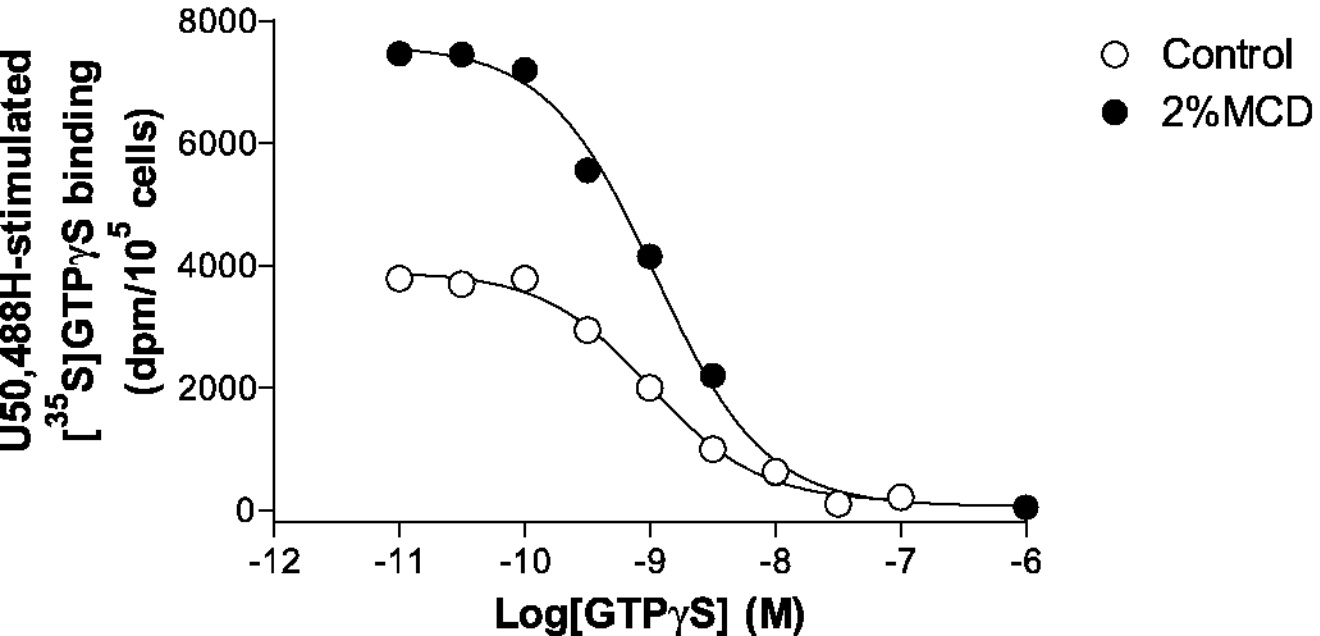

JPET Fast Forward. Published on February 27, 2006 as DOI: 10.1124/jpet.105.099507
This article has not been copyedited and formatted. The final version may differ from this version.

Fig. 7

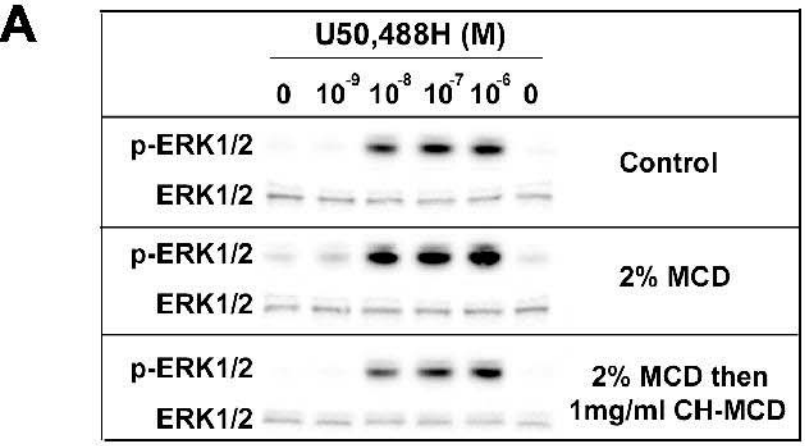

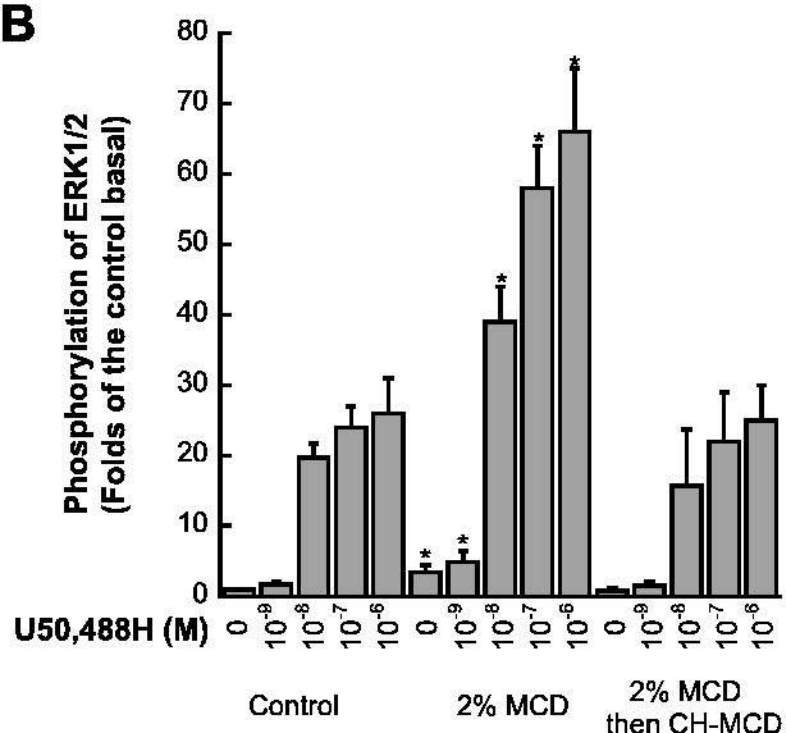

JPET Fast Forward. Published on February 27, 2006 as DOI: 10.1124/jpet.105.099507
This article has not been copyedited and formatted. The final version may differ from this version.

Fig. 8

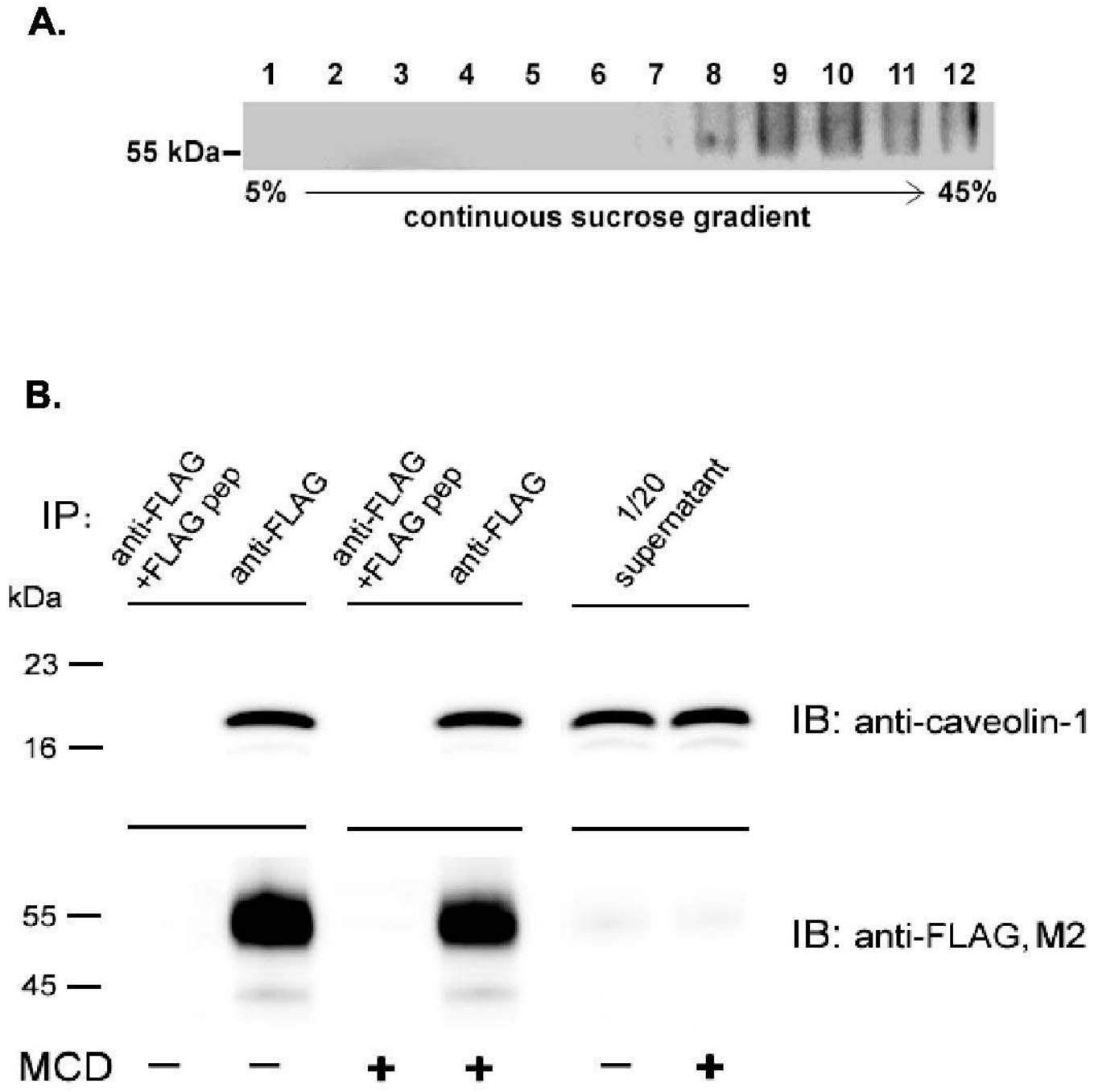

JPET Fast Forward. Published on February 27, 2006 as DOI: 10.1124/jpet.105.099507
This article has not been copyedited and formatted. The final version may differ from this version.

Fig. 9